

Redesigning Lattice QCD

G. Peter Lepage

Newman Laboratory of Nuclear Studies, Cornell University, Ithaca NY 14853

June 27, 2018

Abstract

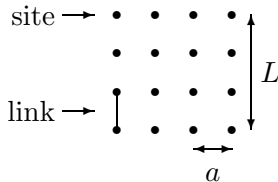
There has been major progress in recent years in the development of improved discretizations of the QCD action, current operators, etc for use in numerical simulations that employ very coarse lattices. These lectures review the field theoretic techniques used to design these discretizations, techniques for testing and tuning the new formalisms that result, and recent simulation results employing these formalisms.

1 Introduction

Lattice quantum chromodynamics is *the* fundamental theory of low-energy strong interactions. In principle, lattice QCD should tell us everything we want to know about hadronic spectra and structure, including such phenomenologically useful things as weak-interaction form factors, decay rates and deep-inelastic structure functions. In these lectures¹ I discuss a revolutionary development that makes the techniques of lattice QCD much more widely accessible and greatly extends the range of problems that are tractable.

The basic approximation in lattice QCD is the replacement of continuous space and time by a discrete grid. The nodes or “sites” of the grid are separated by lattice spacing a , and the length of a side of the grid is L :

¹These lectures were given at the 1996 Schladming Winter School on Perturbative and Nonperturbative Aspects of Quantum Field Theory (Schladming, Austria, March 1996)



The quark and gluon fields from which the theory is built are specified only on the sites of the grid, or on the “links” joining adjacent sites; interpolation is used to find the fields between the sites. In this lattice approximation, the path integral, from which all quantum mechanical properties of the theory can be extracted, becomes an ordinary multidimensional integral where the integration variables are the values of the fields at each of the grid sites:

$$\int \mathcal{D}A_\mu \dots e^{-\int L dt} \longrightarrow \int \prod_{x_j \in \text{grid}} dA_\mu(x_j) \dots e^{-a \sum L_j}. \quad (1)$$

Thus the problem of nonperturbative relativistic quantum field theory is reduced to one of numerical integration. The integral is over a large number of variables and so Monte Carlo methods are generally used in its evaluation. Note that the path integral uses euclidean time rather than ordinary minkowski time, where $t_{\text{eucl}} = I t_{\text{mink}}$; this removes a factor of I from the exponent, getting rid of high-frequency oscillations in the integrand that are hard to integrate.

Early enthusiasm for this approach to nonperturbative QCD gradually gave way to the sobering realization that very large computers would be needed for the numerical integration of the path integral — computers much larger than those that existed in the mid 1970’s, when lattice QCD was invented. Much of a lattice theorist’s effort in the first twenty years of lattice QCD was spent in accumulating computing time on the world’s largest supercomputers, or in designing and building computers far larger than the largest commercially available computers. By the early 1990’s, it was widely felt that teraflop computers costing tens of million of dollars would be essential to the final numerical solution of full QCD.

The revolutionary development I discuss here was the introduction of new techniques that allow one to do realistic numerical simulations of QCD on ordinary desktop workstations or even personal computers. To understand this development one must understand the factors that govern the

cost of a full QCD simulation. This cost is governed by a formula like

$$\text{cost} \propto \left(\frac{L}{a}\right)^4 \left(\frac{1}{a}\right) \left(\frac{1}{m_\pi^2 a}\right) \quad (2)$$

where the first factor is just the number of lattice sites in the grid, and the remaining factors account for the “critical slowing down” of the algorithms used in the numerical integration. This formula shows that the single most important determinant of cost is the lattice spacing. The cost varies as the sixth power of $1/a$, suggesting that one ought to keep the lattice spacing as large as possible. Until very recently it was thought that lattice spacings as small as .05–.1 fm would be essential for reliable simulations of QCD. As I describe in these lectures, new simulation results based on new techniques indicate that spacings as large as .4 fm give accurate results. Assuming that the cost is proportional to $(1/a)^6$, these new simulations using coarse lattices should cost 10^3 – 10^6 times less than traditional simulations on fine lattices.

The computational advantage of coarse lattices is enormous and will certainly redefine numerical QCD: the simplest calculations can be done on a personal computer, while problems of unprecedented difficulty and precision can be tackled with large supercomputers. In these lectures I explain why we now think coarse lattices can be made to work well. I review the techniques from quantum field theory needed to redesign lattice QCD for coarse lattices. These techniques are based on ideas from renormalization theory and effective field theory. I begin in Sect. 2 discussing the field-theoretic implications of discretizing space and time. Then in Sects. 3, 4 and 5 I discuss in detail how to discretize the dynamics of gluons, light quarks and heavy quarks, respectively. I also discuss the crucial issue of testing and tuning improved discretizations. These sections present a mixture of very old and very new results. I do not discuss in any detail the numerical techniques used in the simulations; these are described in standard texts [1, 2, 3]. As these are lectures from a school, I include a number of exercises that illustrate the concepts developed in the lectures. Finally I summarize the current situation and prospects for the future in Sect. 6.

2 Field Theory on a Lattice

In this section I discuss the factors that limit the maximum size of the lattice spacing. Replacing space-time by a discrete lattice is an approximation. If we make the lattice spacing too large, our answers will not be sufficiently

accurate. For the purpose of these lectures, I define a “sufficiently accurate” simulation to be one that reproduces the low-energy properties of hadrons to within a few percent, which is very precise for low-energy strong-interaction physics. The issue then is: How large can we make a while keeping errors of order a few percent or less?

A nonzero lattice spacing results in two types of error: the error that arises when we replace derivatives in the field equations by finite-difference approximations, and the error due to the ultraviolet cutoff imposed by the lattice. I now discuss each of these in turn, and then focus on the key role played by perturbation theory in correcting for finite- a errors.

2.1 Approximate Derivatives

In the lattice approximation, field values are known only at the sites on the lattice. Consequently we approximate derivatives in the field equations by finite-differences that use only field values at the sites. This is completely conventional, and very familiar, numerical analysis. For example, the derivative of a field ψ evaluated at lattice site x_j is approximated by

$$\frac{\partial\psi(x_j)}{\partial x} \approx \Delta_x\psi(x_j) \quad (3)$$

where

$$\Delta_x\psi(x) \equiv \frac{\psi(x+a) - \psi(x-a)}{2a}. \quad (4)$$

It is easy to analyze the error associated with this approximation. Taylor’s Theorem implies that

$$\begin{aligned} 2a \Delta_x\psi(x) &\equiv \psi(x+a) - \psi(x-a) \\ &= \left(e^{a\partial_x} - e^{-a\partial_x} \right) \psi(x) \end{aligned} \quad (5)$$

and therefore

$$\Delta_x\psi = \left(\partial_x + \frac{a^2}{6}\partial_x^3 + \mathcal{O}(a^4) \right) \psi. \quad (6)$$

Thus the relative error in $\Delta_x\psi$ is of order $(a/\lambda)^2$ where λ is the typical length scale in $\psi(x)$.

On coarse lattices we generally need more accurate discretizations than this one. These are easily constructed. For example from (6) it is obvious that

$$\frac{\partial\psi}{\partial x} = \Delta_x\psi - \frac{a^2}{6}\Delta_x^3\psi + \mathcal{O}(a^4), \quad (7)$$

which is a more accurate discretization. When one wishes to reduce the finite- a errors in a simulation, it is usually far more efficient to improve the discretization of the derivatives than to reduce the lattice spacing. For example, with just the first term in the approximation to $\partial_x\psi$, cutting the lattice spacing in half would reduce a 20% error to 5%; but the cost would increase by a factor of $2^6=64$ in a simulation where cost goes like $1/a^6$. On the other hand, including the a^2 correction to the derivative, while working at the larger lattice spacing, achieves the same reduction in error but with a cost increase of only a factor of 2.

Equation 7 shows the first two terms of a systematic expansion of the continuum derivative in powers of a^2 . In principle, higher-order terms can be included to obtain greater accuracy, but in practice the first couple of terms are sufficiently accurate for most purposes. Simple numerical experiments with a^3 -accurate discretizations like this one (see below) show that only three or four lattice sites per bump in ψ are needed to achieve accuracies of a few percent or less. Since ordinary hadrons are approximately 1.8 fm in diameter, these experiments suggest that a lattice spacing of .4 fm would suffice for simulating these hadrons. However QCD is a quantum theory, and, as I discuss in the next section, quantum effects can change everything.

Exercise: Show that

$$\frac{\partial^2\psi}{\partial x^2} = \Delta_x^{(2)}\psi - \frac{a^2}{12} \left(\Delta_x^{(2)}\right)^2 \psi + \mathcal{O}(a^4) \quad (8)$$

where

$$\Delta_x^{(2)}\psi(x) \equiv \frac{\psi(x+a) - 2\psi(x) + \psi(x-a)}{a^2}. \quad (9)$$

Note that Δ_x and $\Delta_x^{(2)}$ can be used to construct lattice approximations for derivatives of any order: for example,

$$\begin{aligned} \Delta_x^{(3)}\psi &\equiv \Delta_x\Delta_x^{(2)}\psi = \Delta^{(2)}\Delta_x\psi \\ &= \partial_x^3\psi + \mathcal{O}(a^2) \end{aligned} \quad (10)$$

$$\begin{aligned} \Delta_x^{(4)}\psi &\equiv \left(\Delta_x^{(2)}\right)^2\psi \\ &= \partial_x^4\psi + \mathcal{O}(a^2) \end{aligned} \quad (11)$$

\vdots

Exercise: Use

$$\psi(x) = e^{-x^2/2\sigma^2} \quad (12)$$

with $\sigma = 2a$ as a sample function to test our discretizations of $\partial_x\psi$ and $\partial_x^2\psi$. Evaluate the a^2 errors of the simplest discretization in each case, and the a^4

errors of the more accurate discretizations. Show that the a^2 errors are of order 10–20%, while the a^4 errors are only a few percent or less. Note that $\Delta^{(2)}$ is more substantially more accurate than $\Delta^{(1)}$.

2.2 Ultraviolet Cutoff

The shortest wavelength oscillation that can be modeled on a lattice is one with wavelength $\lambda_{\min} = 2a$; for example, the function $\psi(x) = +1, -1, +1 \dots$ for $x = 0, a, 2a \dots$ oscillates with this wavelength. Thus gluons and quarks with momenta $k = 2\pi/\lambda$ larger than π/a are excluded from the lattice theory by the lattice; that is, the lattice functions as an ultraviolet cutoff. In simple classical field theories this is often irrelevant: short-wavelength ultraviolet modes are either unexcited or decouple from the long-wavelength infrared modes of interest. However, in a noisy nonlinear theory, like an interacting quantum field theory, ultraviolet modes strongly affect infrared modes by renormalizing masses and interactions. Thus we cannot simply discard all particles with momenta larger than π/a ; we must somehow mimic their effects on infrared states. This we can do by modifying our discretized lagrangian.²

To see how we might mimic the effects of $k > \pi/a$ states on low momentum states, consider the scattering amplitude T for quark-quark scattering in one-loop perturbation theory (Fig. 1a). The difference between the correct amplitude T in the continuum theory and the cut-off amplitude $T^{(a)}$ in our lattice theory involves internal gluons with momentum k of order π/a or larger. This is because the classical theories agree at low momenta, and therefore all propagators and vertices agree there as well. Thus the loop contributions from low momenta will be the same in T and $T^{(a)}$, and cancel in the difference. Given that the external quarks have momenta p_i that are small relative to π/a , we can expand the difference $T - T^{(a)}$ in a Taylor series in $a p_i$ to obtain

$$\begin{aligned}
 T - T^{(a)} &= a^2 c(a) \bar{u}(p_2) \gamma_\mu u(p_1) \bar{u}(p_4) \gamma^\mu u(p_3) \\
 &+ a^2 c_A(a) \bar{u} \gamma_\mu \gamma_5 u \bar{u} \gamma^\mu \gamma_5 u \\
 &+ a^4 d(a) (p_1 - p_2)^2 \bar{u} \gamma_\mu u \bar{u} \gamma^\mu u \\
 &+ \dots
 \end{aligned} \tag{13}$$

²The idea of modifying the lagrangian to compensate for a finite UV cutoff is central to chiral field theories for pions, nonrelativistic QED/QCD and all other effective field theories. The application to lattice field theories was pioneered in the form discussed here by Symanzik and is referred to as ‘‘Symanzik improvement’’ of lattice operators [4].

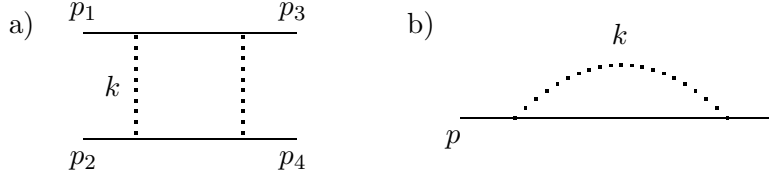


Figure 1: One-loop amplitudes contributing to: a) $qq \rightarrow qq$, and b) the quark self energy.

where the couplings c , $c_A \dots$ are dimensionless functions of the cutoff. This difference is what is missing from the lattice theory; it is the contribution of the $k > \pi/a$ states excluded by the lattice.³ The key observation is that we can reintroduce this high- k contribution into the lattice theory by adding new interactions to the lattice lagrangian:

$$\begin{aligned}
\delta\mathcal{L}_{4q}^{(a)} &= \frac{1}{2} a^2 c(a) \bar{\psi}\gamma_\mu\psi \bar{\psi}\gamma^\mu\psi \\
&+ \frac{1}{2} a^2 c_A(a) \bar{\psi}\gamma_\mu\gamma_5\psi \bar{\psi}\gamma^\mu\gamma_5\psi \\
&+ a^4 d(a) \bar{\psi}D^2\gamma_\mu\psi \bar{\psi}\gamma^\mu\psi \\
&+ \dots
\end{aligned} \tag{14}$$

These new local interactions give the same contribution to $T(qq \rightarrow qq)$ in the lattice theory as the $k > \pi/a$ states do in the continuum theory. Although these correction terms are nonrenormalizable, they do not cause problems in our lattice theory because it is cut off at π/a . On the contrary, they bring our lattice theory closer to the continuum without reducing the lattice spacing.

This simple analysis illustrates a general result of renormalization theory: one can mimick the effects of states excluded by a cutoff with extra local interactions in the cut-off lagrangian. The correction terms in $\delta\mathcal{L}^{(a)}$ are all local—that is, they are polynomials in the fields and in derivatives of the fields—since contributions omitted as a consequence of the cutoff can be Taylor-expanded in powers of ap_i . This is intuitively reasonable since these terms correct for contributions from intermediate states that are highly virtual and thus quite local in extent; the locality is a consequence of the uncertainty principle. The relative importance of the different interactions

³More precisely, this contribution is due to states above the cutoff, and to corrections needed to fix up the states below but sufficiently near the cutoff that they suffer severe lattice distortion.

is determined by the number of powers of a in their coefficients, and that is determined by the dimensions of the operators involved: each term in $\delta\mathcal{L}^{(a)}$ must have total (energy) dimension four, and so if the operator in a particular term has dimension $n + 4$ then the coefficient must contain a factor a^n . In principle there are infinitely many correction terms, but we need only include interactions with operators of dimension $n + 4$ or less to achieve accuracy through order $(ap_i)^n$. In practice we only need precision to a given order n in ap_i , and there are only a finite number of local operators with dimension less than or equal to any given $n + 4$.

Initially the $k > \pi/a$ contributions appear to be bad news. As we argued in the previous section, a^2 corrections are necessary for precision when a is large. However the quantum nature of our theory implies that there are a^2 terms, due to $k > \pi/a$ states, which depend in detail on the nature of the theory. Thus, for example, when we discretize the derivative in the QCD quark action we replace

$$\bar{\psi}\partial \cdot \gamma\psi \rightarrow \bar{\psi}\Delta \cdot \gamma\psi + a^2 d(a)\bar{\psi}\Delta^{(3)} \cdot \gamma\psi + \dots \quad (15)$$

where now $d(a)$ has a part, $-1/6$, from numerical analysis (equation (7)) plus a contribution that mimicks the $k > \pi/a$ part of the quark self energy (Fig. 1b). The problem is that the latter contribution is, by its nature, completely theory specific; we cannot look it up in a book on numerical analysis. We must somehow solve the $k > \pi/a$ part of the field theory in order to calculate it; otherwise we are unable to correct our lagrangian and unable to use large lattice spacings.

The good news, for lattice QCD, is that $k > \pi/a$ QCD is perturbative provided a is small enough (because of asymptotic freedom). Then correction coefficients like $d(a)$ can be computed perturbatively, using Feynman diagrams, in an expansion in powers of $\alpha_s(\pi/a)$. Thus, for example, our corrected lattice action for quarks becomes

$$\begin{aligned} \mathcal{L}^{(a)} &= \bar{\psi}(\Delta \cdot \gamma + m(a))\psi \\ &+ d(a)a^2\bar{\psi}\Delta^{(3)} \cdot \gamma\psi \\ &+ c(a)a^2\bar{\psi}\gamma_\mu\psi\bar{\psi}\gamma^\mu\psi + \dots \end{aligned} \quad (16)$$

where

$$d(a) = -\frac{1}{6} + d_1\alpha_s(\pi/a) + \dots \quad (17)$$

$$c(a) = c_2\alpha_s^2(\pi/a) + \dots \quad (18)$$

...

are computed to whatever order in perturbation theory is necessary. In this way we use perturbation theory to, in effect, fill in the gaps between lattice points, allowing us to obtain continuum results without taking the lattice spacing to zero.

2.3 Perturbation Theory and Tadpole Improvement⁴

Improved discretizations and large lattice spacings are old ideas, pioneered by Wilson, Symanzik and others [6]. However, perturbation theory is essential; the lattice spacing a must be small enough so that $k \approx \pi/a$ QCD is perturbative. This was the requirement that drove lattice QCD towards very costly simulations with tiny lattice spacings. Traditional perturbation theory for lattice QCD begins to fail at distances of order 1/20 to 1/10 fm, and therefore lattice spacings must be at least this small before improved actions are useful. This seems very odd since phenomenological applications of continuum perturbative QCD suggest that perturbation theory works well down to energies of order 1 GeV, which corresponds to a lattice spacing of 0.6 fm. The breakthrough, in the early 1990's, was the discovery of a trivial modification of lattice QCD, called "tadpole improvement," that allows perturbation theory to work even at distances as large as 1/2 fm [5, 7].

One can readily derive Feynman diagram rules for lattice QCD using the same techniques as in the continuum, but applied to the lattice lagrangian [8]. The particle propagators and interaction vertices are usually complicated functions of the momenta that become identical to their continuum analogues in the low-momentum limit. All loop momenta are cut off at $k_\mu = \pm\pi/a$.

Testing perturbation theory is also straightforward. One designs short-distance quantities that can be computed easily in a simulation (i.e., in a Monte Carlo evaluation of the lattice path integral). The Monte Carlo gives the exact value which can then be compared with the perturbative expansion for the same quantity. An example of such a quantity is the expectation value of the Wilson loop operator,

$$W(\mathcal{C}) \equiv \langle 0 | \frac{1}{3} \text{Re Tr P} e^{-ig \oint_{\mathcal{C}} A \cdot dx} | 0 \rangle, \quad (19)$$

where A is the QCD vector potential, P denotes path ordering, and \mathcal{C} is any small, closed path or loop on the lattice. $W(\mathcal{C})$ is perturbative for sufficiently small loops \mathcal{C} . We can test the utility of perturbation theory over any range

⁴This section is based upon work with Paul Mackenzie that is described in [5].

of distances by varying the loop size while comparing numerical Monte Carlo results for $W(\mathcal{C})$ with perturbation theory.

Fig. 2 illustrates the highly unsatisfactory state of traditional lattice-QCD perturbation theory. There I show the “Creutz ratio” of $2a \times 2a$, $2a \times a$ and $a \times a$ Wilson loops,

$$\chi_{2,2} \equiv -\ln \left(\frac{W(2a \times 2a) W(a \times a)}{W^2(2a \times a)} \right), \quad (20)$$

plotted versus the size $2a$ of the largest loop. Traditional perturbation theory (dotted lines) underestimates the exact result by factors of three or four for loops of order 1/2 fm; only when the loops are smaller than 1/20 fm does perturbation theory begin to give accurate results.

The problem with traditional lattice-QCD perturbation theory is that the coupling it uses is much too small. The standard practice was to express perturbative expansions of short-distance lattice quantities in terms of the bare coupling α_{lat} used in the lattice lagrangian. This practice followed from the notion that the bare coupling in a cutoff theory is approximately equal to the running coupling evaluated at the cutoff scale, here $\alpha_s(\pi/a)$, and therefore that it is the appropriate coupling for quantities dominated by momenta near the cutoff. In fact the bare coupling in traditional lattice QCD is much smaller than true effective coupling at large lattice spacings: for example,

$$\alpha_{\text{lat}} = \alpha_V(\pi/a) - 4.7 \alpha_V^2 + \dots \quad (21)$$

$$\leq \frac{1}{2} \alpha_V(\pi/a) \quad \text{for } a > .1 \text{ fm} \quad (22)$$

where $\alpha_V(q)$ is a continuum coupling defined by the static-quark potential,

$$V_{\text{Q}\bar{\text{Q}}}(q) \equiv -4 \pi C_F \frac{\alpha_V(q)}{q^2}. \quad (23)$$

Consequently α_{lat} expansions, though formally correct, badly underestimate perturbative effects, and converge poorly.

The anomalously small bare coupling in the traditional lattice theory is a symptom of the “tadpole problem”. As we discuss later, all gluonic operators in lattice QCD are built from the link operator

$$U_\mu(x) \equiv \text{P} e^{-\int_x^{x+a\hat{\mu}} gA \cdot dx} \approx e^{-IagA_\mu} \quad (24)$$

rather than from the vector potential A_μ . Thus, for example, the leading term in the lagrangian that couples quarks and gluons is $\bar{\psi} U_\mu \gamma_\mu \psi / a$. Such

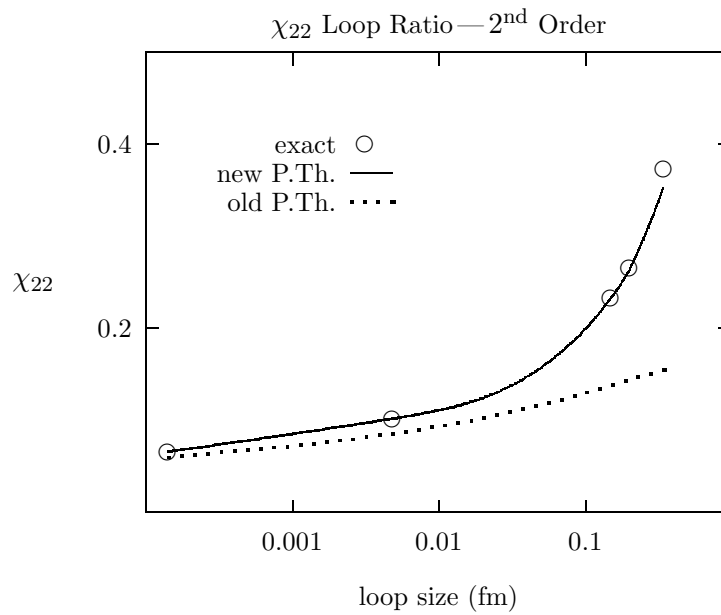
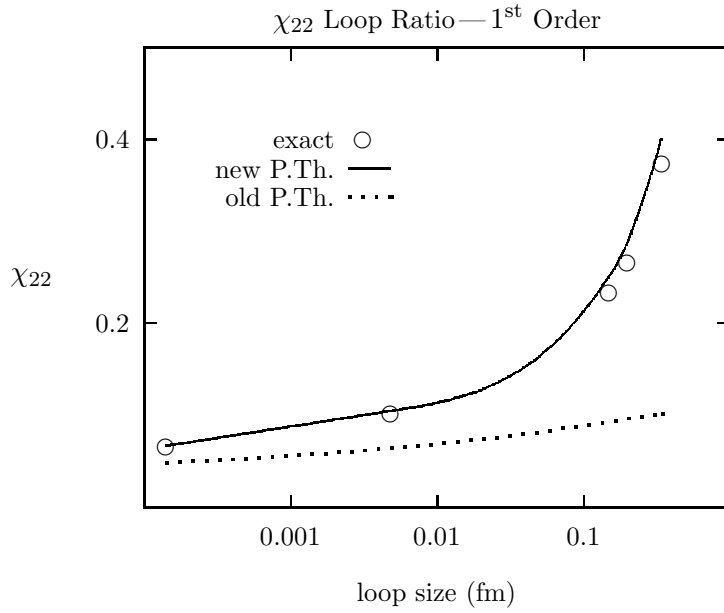


Figure 2: The χ_{22} Creutz ratio of Wilson loops versus loop size. Results from Monte Carlo simulations (exact), and from tadpole-improved (new) and traditional (old) lattice perturbation theory are shown.

a term contains the usual $\bar{\psi}gA \cdot \gamma\psi$ vertex, but, in addition, it contains vertices with any number of additional powers of agA_μ . These extra vertices are irrelevant for classical fields since they are suppressed by powers of the lattice spacing. For quantum fields, however, the situation is quite different since pairs of A_μ 's, if contracted with each other, generate ultraviolet divergent factors of $1/a^2$ that precisely cancel the extra a 's. Consequently the contributions generated by the extra vertices are suppressed by powers of g^2 (not a), and turn out to be uncomfortably large. These are the tadpole contributions.

The tadpoles result in large renormalizations — often as large as a factor of two or three — that spoil naive perturbation theory, and with it our intuition about the connection between lattice operators and the continuum. However tadpole contributions are generically process independent and so it is possible to measure their contribution in one quantity and then correct for them in all other quantities.

The simplest way to do this is to cancel them out. The mean value u_0 of $\frac{1}{3} \text{Re Tr } U_\mu$ consists of only tadpoles and so we can largely cancel the tadpole contributions by dividing every link operator by u_0 . That is, in every lattice operator we replace

$$U_\mu(x) \rightarrow \frac{U_\mu(x)}{u_0} \quad (25)$$

where u_0 is computed numerically in a simulation.

The u_0 's cancel tadpole contributions, making lattice operators and perturbation theory far more continuum-like in their behavior. Thus, for example, the only change in the standard gluon action when it is tadpole-improved is that the new bare coupling α_{TI} is enhanced by a factor of $1/u_0^4$ relative to the coupling α_{lat} in the unimproved theory:

$$\alpha_{\text{TI}} = \frac{\alpha_{\text{lat}}}{u_0^4}. \quad (26)$$

Since $u_0^4 < .6$ when $a > .1$ fm, the tadpole-improved coupling is typically more than twice as large for coarse lattices. Expressing α_{TI} in terms of the continuum coupling α_V , we find that now our intuition is satisfied:

$$\alpha_{\text{TI}} = \alpha_V(\pi/a) - .5\alpha_V^2 + \dots \quad (27)$$

$$\approx \alpha_V(\pi/a). \quad (28)$$

Perturbation theory for the Creutz ratio (20) converges rapidly to the correct answer when it is reexpressed in terms of α_{TI} . An even better result

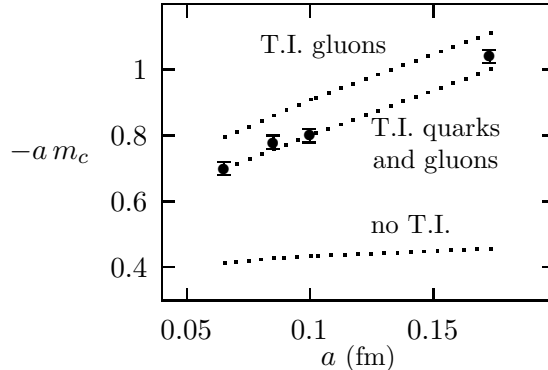


Figure 3: The critical bare quark mass for Wilson’s lattice quark action versus lattice spacing. Monte Carlo data points are compared with perturbation theories in a theory with no tadpole improvement (T.I), tadpole-improved gluon dynamics, and tadpole-improved quark and gluon dynamics.

is obtained if the expansion is reexpressed as a series in a coupling constant defined in terms of a physical quantity, like the static-quark potential, where that coupling constant is measured in a simulation. By measuring the coupling we automatically include any large renormalizations of the coupling due to tadpoles. It is important that the scale q^* at which the running coupling constant is evaluated be chosen appropriately for the quantity being studied [5, 7]. When these refinements are added, perturbation theory is dramatically improved, and, as illustrated in Fig. 2, is still quite accurate for loops as large as 1/2 fm.

This same conclusion follows from Fig. 3 which shows the value of the bare quark mass needed to obtain zero-mass pions using Wilson’s lattice action for quarks. This quantity diverges linearly as the lattice spacing vanishes, and so should be quite perturbative. Here we see dramatic improvements as the tadpoles are removed first from the gluon action, through use of an improved coupling, and then also from the quark action.

The Creutz ratio and the critical quark mass are both very similar to the couplings we need to compute for improved lagrangians. Tadpole improvement has been very successful in a wide range of applications.

Exercise: Derive the Feynman rules for lattice ϕ^4 theory where

$$S = \sum_x a^4 \left\{ \frac{-\phi \Delta^{(2)} \phi + m^2 \phi^2}{2} + \frac{\lambda \phi^4}{4!} \right\}. \quad (29)$$

In particular show that the ϕ propagator is

$$G \propto \frac{a^2}{\sum_\mu (2 \sin(ap_\mu/2))^2 + a^2 m^2} \quad (30)$$

2.4 An Aside on “Perfect Actions”

Although not necessary in practice, it is possible to sum all the terms in the a^2 expansion of a continuum derivative using Fourier transforms: for example, we replace

$$\partial_x^2 \psi(x_i) \rightarrow - \sum_j d_{\text{pf}}^{(2)}(x_i - x_j) \psi(x_j) \quad (31)$$

where

$$d_{\text{pf}}^{(2)}(x_i - x_j) \equiv \int \frac{dp}{2\pi} p^2 e^{Ip(x_i - x_j)} \theta(|p| < \pi/a). \quad (32)$$

We do not do this because $d_{\text{pf}}^{(2)}(x_i - x_j)$ falls off only as $1/|x_i - x_j|^2$ for large $|x_i - x_j|$, resulting in highly nonlocal actions and operators that are very costly to simulate, particularly when gauge fields are involved. So it is generally far better to truncate the a^2 expansion than to sum to all orders. However this analysis suggests a different strategy for discretization that we now examine.

The slow fall-off in the all-orders or perfect derivative $d_{\text{pf}}^{(2)}$ is caused by the abruptness of the lattice cutoff (the θ function in (32)). Wilson noticed that $d^{(2)}$ can be made to vanish faster than any power of $1/|x_i - x_j|$ if a smoother cutoff is introduced. In his approach the lattice field at node x_i is *not* equal to the continuum field there, but rather equals the continuum field averaged over a small volume centered at that node: for example, the lattice field at site x_i in one dimension is⁵

$$\Psi_i = \frac{1}{a} \int_{x_i - a/2}^{x_i + a/2} \psi(x) dx \quad (33)$$

⁵The smearing discussed here is conceptually simple, but better smearings, resulting in improved locality, are possible. In [9] the authors use stochastic smearing in which Ψ_i equals the blocked continuum field only on average. This introduces a new parameter that can be tuned to optimize the action.

$$= \int_{-\infty}^{\infty} \frac{dp}{2\pi} e^{Ip x_i} \Pi(p) \psi(p) \quad (34)$$

where, in the transform, smearing function

$$\Pi(p) \equiv \frac{2 \sin(pa/2)}{pa} \quad (35)$$

provides a smooth cutoff at large p . The lattice action for the smeared fields is designed so that tree-level Green's functions built from these fields are *exactly* equal to the corresponding Green's functions in the continuum theory, with the smearing function applied at the ends: for example,

$$\langle \Psi_i \Psi_j \rangle = \int_{x_i-a/2}^{x_i+a/2} dx \int_{x_j-a/2}^{x_j+a/2} dy \langle \psi(x) \psi(y) \rangle \quad (36)$$

$$= \int_{-\infty}^{\infty} \frac{dp}{2\pi} e^{Ip(x_i-x_j)} \frac{\Pi^2(p)}{p^2 + m^2}. \quad (37)$$

By rewriting the propagator $\langle \Psi_i \Psi_j \rangle$ in the form

$$\int_{-\pi/a}^{\pi/a} \frac{dp}{2\pi} e^{Ip(x_i-x_j)} \sum_n \frac{\Pi^2(p+2\pi n/a)}{(p+2\pi n/a)^2 + m^2}, \quad (38)$$

we find that the quadratic terms of this lattice action are

$$S^{(2)} = \frac{1}{2} \sum_{i,j} \Psi_i d_{\text{pa}}^{(2)}(x_i - x_j, m) \Psi_j, \quad (39)$$

where $d_{\text{pa}}^{(2)}(x_i - x_j, m)$ is

$$\int_{-\pi/a}^{\pi/a} \frac{dp}{2\pi} e^{Ip(x_i-x_j)} \left(\sum_n \frac{\Pi^2(p+2\pi n/a)}{(p+2\pi n/a)^2 + m^2} \right)^{-1}. \quad (40)$$

It is easily shown that, remarkably, $d_{\text{pa}}^{(2)}(x_i - x_j, m)$ vanishes faster than any power of $1/|x_i - x_j|$ as the separation increases. So the derivative terms in such an action are both exact to all orders in a and quite local—that is, the classical action is “perfect.” Again, this is possible because the lattice field Ψ_i is obtained by smearing the continuum field, which introduces a smooth UV cutoff in momentum space rather than the abrupt cutoff of (32).

The complication with this approach is that it is difficult to reconstruct the continuum fields $\psi(x)$ from the smeared lattice fields Ψ_i . Consequently

nonlinear interactions, currents, and other operators are generally complicated functions of the Ψ_i , and much more difficult to design than with the previous approach, where the lattice field is trivially related to the continuum field. This is an important issue in QCD where phenomenological studies involve a wide range of currents and operators. It also means that in practice the “perfect action” used for an interacting theory is not really perfect since the arbitrarily complex functions of Ψ_i that arise in real perfect actions must be simplified for simulations. Although these difficulties gradually are being overcome for QCD [10, 11], I will not discuss this interesting approach further in these lectures.

2.5 Summary

Asymptotic freedom implies that short-distance QCD is simple (perturbative) while long-distance QCD is difficult (nonperturbative). The lattice separates short from long distances, allowing us to exploit this dichotomy to create highly efficient algorithms for solving the entire theory: $k > \pi/a$ QCD is included via corrections $\delta\mathcal{L}$ to the lattice lagrangian that are computed using perturbation theory; $k < \pi/a$ QCD is handled nonperturbatively using Monte Carlo integration. Thus, while we wish to make the lattice spacing a as large as possible, we are constrained by two requirements. First a must be sufficiently small that our finite-difference approximations for derivatives in the lagrangian and field equations are sufficiently accurate. Second a must be sufficiently small that π/a is a perturbative momentum. Numerical experiments indicate that both constraints can be satisfied when $a \approx 1/2$ fm or smaller, provided all lattice operators are tadpole improved.

It is important to remember that most any perturbative analysis in QCD is contaminated by nonperturbative effects at some level. This will certainly be the case for the couplings in $\delta\mathcal{L}$. However we now have extensive experience showing that such nonperturbative effects are rarely significant for physical quantities at the distances relevant to our discussion. Should a situation arise where this is not the case (and one surely will, some day) we may have to supplement the perturbative approach outlined in this section with nonperturbative techniques. Such situations will not pose a problem if they are relatively rare, as now seems likely. Furthermore, as we discuss later, simple nonperturbative techniques already exist, should they be needed, for tuning the leading correction terms in both the gluon and quark actions.

3 Gluon Dynamics on Coarse Lattices

In this section I discuss first the construction of accurate discretizations of the classical theory of gluon dynamics. I then discuss the changes needed to make a quantum theory, and illustrate the discussion with Monte Carlo results. Finally I discuss actions for anisotropic lattices, and the tuning and testing of gluon actions.

3.1 Classical Gluons

The continuum action for QCD is

$$S = \int d^4x \frac{1}{2} \sum_{\mu, \nu} \text{Tr} F_{\mu\nu}^2(x) \quad (41)$$

where

$$F_{\mu\nu} \equiv \partial_\mu A_\nu - \partial_\nu A_\mu + ig[A_\mu, A_\nu] \quad (42)$$

is the field tensor, a traceless 3×3 hermitian matrix. The defining characteristic of the theory is its invariance with respect to gauge transformations where

$$F_{\mu\nu} \rightarrow \Omega(x) F_{\mu\nu} \Omega(x)^\dagger \quad (43)$$

and $\Omega(x)$ is an arbitrary x -dependent SU_3 matrix.

The standard discretization of this theory seems perverse at first sight. Rather than specifying the gauge field by the values of $A_\mu(x)$ at the sites of the lattice, the field is specified by variables on the links joining the sites. In the classical theory, the “link variable” on the link joining a site at x to one at $x + a\hat{\mu}$ is determined by the line integral of A_μ along the link:

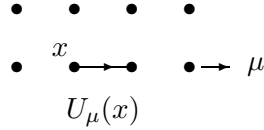
$$U_\mu(x) \equiv \text{P exp} \left(-i \int_x^{x+a\hat{\mu}} gA \cdot dy \right) \quad (44)$$

where the P-operator path-orders the A_μ 's along the integration path. We use U_μ 's in place of A_μ 's on the lattice, because it is impossible to formulate a lattice version of QCD directly in terms of A_μ 's that has exact gauge invariance. The U_μ 's, on the other hand, transform very simply under a gauge transformation:

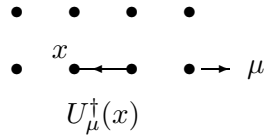
$$U_\mu(x) \rightarrow \Omega(x) U_\mu(x) \Omega(x + a\hat{\mu})^\dagger. \quad (45)$$

This makes it easy to build a discrete theory with exact gauge invariance.

A link variable $U_\mu(x)$ is represented pictorially by a directed line from x to $x + \hat{\mu}$, where this line is the integration path for the line integral in the exponent of $U_\mu(x)$:



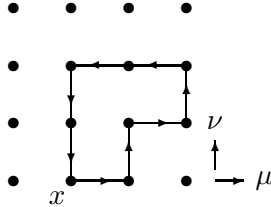
In the conjugate matrix $U_\mu^\dagger(x)$ the direction of the line integral is flipped and so we represent $U_\mu^\dagger(x)$ by a line going backwards from $x + \hat{\mu}$ to x :



A Wilson loop function,

$$W(\mathcal{C}) \equiv \frac{1}{3} \text{Tr} \text{P} e^{-i \oint_{\mathcal{C}} g A \cdot dx}, \quad (46)$$

for any closed path \mathcal{C} built of links on the lattice can be computed from the path-ordered product of the U_μ 's and U_μ^\dagger 's associated with each link. For example, if \mathcal{C} is the loop



then

$$W(\mathcal{C}) = \frac{1}{3} \text{Tr} \left(U_\mu(x) U_\nu(x + a\hat{\mu}) \dots U_\nu^\dagger(x) \right). \quad (47)$$

Such quantities are obviously invariant under arbitrary gauge transformations (45).

You might wonder why we go to so much trouble to preserve gauge invariance when we quite willing give up Lorentz invariance, rotation invariance, etc. The reason is quite practical. With gauge invariance, the

quark-gluon, three-gluon, and four-gluon couplings in QCD are all equal, and the bare gluon mass is zero. Without gauge invariance, each of these couplings must be tuned independently and a gluon mass introduced if one is to recover QCD. Tuning this many parameters in a numerical simulation is very expensive. This is not much of a problem in the classical theory, where approximate gauge invariance keeps the couplings approximately equal; but it is serious in the quantum theory because quantum fluctuations (loop-effects) renormalize the various couplings differently in the absence of exact gauge invariance. So while it is quite possible to formulate lattice QCD directly in terms of A_μ 's, the resulting theory would have only approximate gauge invariance, and thus would be prohibitively expensive to simulate. Symmetries like Lorentz invariance can be given up with little cost because the symmetries of the lattice, though far less restrictive, are still sufficient to prevent the introduction of new interactions with new couplings (at least to lowest order in a).

We must now build a lattice lagrangian from the link operators. We require that the lagrangian be gauge invariant, local, and symmetric with respect to axis interchanges (which is all that is left of Lorentz invariance). The most local nontrivial gauge invariant object one can build from the link operators is the ‘‘plaquette operator,’’ which involves the product of link variables around the smallest square at site x in the $\mu\nu$ plane:

$$P_{\mu\nu}(x) \equiv \frac{1}{3} \text{Re Tr} \left(U_\mu(x) U_\nu(x + a\hat{\mu}) U_\mu^\dagger(x + a\hat{\mu} + a\hat{\nu}) U_\nu^\dagger(x) \right). \quad (48)$$

To see what this object is, consider evaluating the plaquette centered about a point x_0 for a very smooth weak classical A_μ field. In this limit,

$$P_{\mu\nu} \approx 1 \quad (49)$$

since

$$U_\mu \approx e^{-IgaA_\mu} \approx 1. \quad (50)$$

Given that A_μ is slowly varying, its value anywhere on the plaquette should be accurately specified by its value and derivatives at x_0 . Thus the corrections to (49) should be a polynomial in a with coefficients formed from gauge-invariant combinations of $A_\mu(x_0)$ and its derivatives: that is,

$$\begin{aligned} P_{\mu\nu} = 1 & - c_1 a^4 \text{Tr} (gF_{\mu\nu}(x_0))^2 \\ & - c_2 a^6 \text{Tr} \left(gF_{\mu\nu}(x_0) (D_\mu^2 + D_\nu^2) gF_{\mu\nu}(x_0) \right) \\ & + \mathcal{O}(a^8) \end{aligned} \quad (51)$$

where c_1 and c_2 are constants, and D_μ is the gauge-covariant derivative. The leading correction is order a^4 because $F_{\mu\nu}^2$ is the lowest-dimension gauge-invariant combination of derivatives of A_μ , and it has dimension 4. (There are no F^3 terms because $P_{\mu\nu}$ is invariant under $U_\mu \rightarrow U_\mu^\dagger$ or, equivalently, $F \rightarrow -F$.)

It is straightforward to find the coefficients c_1 and c_2 . We need only examine terms in the expansion of $P_{\mu\nu}$ that are quadratic in A_μ ; the cubic and quartic parts of $F_{\mu\nu}^2$ then follow automatically, by gauge invariance. Because of the trace, the path ordering is irrelevant to this order. Thus

$$\begin{aligned} P_{\mu\nu} &= \frac{1}{3} \text{Re Tr P e}^{-i \oint_{\square} gA \cdot dx} \\ &= \frac{1}{3} \text{Re Tr} \left[1 - i \oint_{\square} gA \cdot dx - \frac{1}{2} \left(\oint_{\square} gA \cdot dx \right)^2 + \mathcal{O}(A^3) \right] \end{aligned} \quad (52)$$

where, by Stoke's Theorem,

$$\begin{aligned} \oint_{\square} A \cdot dx &= \int_{-a/2}^{a/2} dx_\mu dx_\nu [\partial_\mu A_\nu(x_0 + x) - \partial_\nu A_\mu(x_0 + x)] \\ &= \int_{-a/2}^{a/2} dx_\mu dx_\nu [F_{\mu\nu}(x_0) + (x_\mu D_\mu + x_\nu D_\nu)F_{\mu\nu}(x_0) + \dots] \\ &= a^2 F_{\mu\nu}(x_0) + \frac{a^4}{24} (D_\mu^2 + D_\nu^2)F_{\mu\nu}(x_0) + \mathcal{O}(a^6, A^2). \end{aligned} \quad (53)$$

Thus $c_1 = 1/6$ and $c_2 = 1/72$ in (51).

The expansion in (51) is the classical analogue of an operator product expansion. Using this expansion, we find that the traditional ‘‘Wilson action’’ for gluons on a lattice,

$$S_{\text{Wil}} = \beta \sum_{x, \mu > \nu} (1 - P_{\mu\nu}(x)) \quad (54)$$

where $\beta = 6/g^2$, has the correct limit for small lattice spacing up to corrections of order a^2 :

$$S_{\text{Wil}} = \int d^4x \sum_{\mu, \nu} \left\{ \frac{1}{2} \text{Tr } F_{\mu\nu}^2 + \frac{a^2}{24} \text{Tr } F_{\mu\nu} (D_\mu^2 + D_\nu^2) F_{\mu\nu} + \dots \right\}. \quad (55)$$

We can cancel the a^2 error in the Wilson action by adding other Wilson loops. For example, the $2a \times a$ ‘‘rectangle operator’’

$$R_{\mu\nu} = \frac{1}{3} \text{Re Tr} \left[\begin{array}{c} \boxed{\begin{array}{ccc} \rightarrow & & \rightarrow \\ \leftarrow & & \leftarrow \\ \leftarrow & & \leftarrow \\ \rightarrow & & \rightarrow \end{array}} \begin{array}{c} \nu \\ \uparrow \\ \mu \end{array} \end{array} \right] \quad (56)$$

has expansion

$$R_{\mu\nu} = 1 - \frac{4}{6} a^4 \text{Tr} (gF_{\mu\nu})^2 - \frac{4}{72} a^6 \text{Tr} \left(gF_{\mu\nu} (4D_\mu^2 + D_\nu^2) gF_{\mu\nu} \right) - \dots \quad (57)$$

The mix of a^4 terms and a^6 terms in the rectangle is different from that in the plaquette. Therefore we can combine the two operators to obtain an improved classical lattice action that is accurate up to $\mathcal{O}(a^4)$ [12, 13]:

$$S_{\text{classical}} \equiv -\beta \sum_{x,\mu>\nu} \left\{ \frac{5P_{\mu\nu}}{3} - \frac{R_{\mu\nu} + R_{\nu\mu}}{12} \right\} + \text{const} \quad (58)$$

$$= \int d^4x \sum_{\mu,\nu} \frac{1}{2} \text{Tr} F_{\mu\nu}^2 + \mathcal{O}(a^4). \quad (59)$$

This process is the analogue of improving the derivatives in discretizations of non-gauge theories.⁶

Exercise: The euclidean Green's function or propagator G for a nonrelativistic quark in a background gauge field A_μ satisfies the equation

$$\left(D_t - \frac{\mathbf{D}^2}{2M} \right) G(x) = \delta^4(x) \quad (60)$$

where $D_\mu = \partial_\mu - igA_\mu(x)$ is the gauge-covariant derivative. Show that the static ($M = \infty$) quark propagator is

$$G_\infty(\mathbf{x}, t) = \left[\text{P e}^{-i \int_0^t gA_0(\mathbf{x}, t) dt} \right]^\dagger \delta^3(\mathbf{x}) \quad (61)$$

which on the lattice becomes

$$G_\infty(\mathbf{x}, t) = U_t^\dagger(\mathbf{x}, t-a) U_t^\dagger(\mathbf{x}, t-2a) \dots U_t^\dagger(\mathbf{x}, 0). \quad (62)$$

Propagation of a static antiquark is described by G_∞^\dagger and therefore the “static potential” $V(r)$, which is the energy of a static quark and antiquark a distance r apart, is obtained from

$$W(r, t) \equiv \langle 0 | \frac{1}{3} \text{Tr} \left[\begin{array}{c} \text{---} \bullet \text{---} \bullet \text{---} \bullet \text{---} \\ \bullet \quad \bullet \quad \bullet \\ \text{---} \bullet \text{---} \bullet \text{---} \bullet \text{---} \end{array} \right] | 0 \rangle \quad \begin{array}{l} \uparrow \\ r \\ \downarrow \end{array} \quad (63)$$

← t →

⁶An important step that I have not discussed is to show that the gluon action is positive for any configuration of link variables. This guarantees that the classical ground state of the lattice action corresponds to $F_{\mu\nu} = 0$. See [13] for a detailed discussion.

The expectation value of the link operator is gauge dependent. Thus to minimize gauge artifacts, u_0 is commonly defined as the Landau-gauge expectation value, $\langle 0 | \frac{1}{3} \text{Tr} U_\mu | 0 \rangle_{\text{LG}}$. Landau gauge is the axis-symmetric gauge that maximizes u_0 , thereby minimizing the tadpole contribution; any tadpole contribution that is left in Landau gauge cannot be a gauge artifact. An alternative procedure is to define u_0 as the fourth root of the plaquette expectation value,

$$u_0 = \langle 0 | P_{\mu\nu} | 0 \rangle^{1/4}. \quad (69)$$

This definition gives almost identical results and is more convenient for numerical work since gauge fixing is unnecessary.

Tadpole improvement is the first step in a systematic procedure for improving the action. The next step is to add in renormalizations due to contributions from $k > \pi/a$ physics not already included in the tadpole improvement. These renormalizations induce $a^2 \alpha_s (\pi/a)$ corrections,

$$\begin{aligned} \delta\mathcal{L} &= \alpha_s r_1 a^2 \sum_{\mu,\nu} \text{Tr}(F_{\mu\nu} D_\mu^2 F_{\mu\nu}) \\ &+ \alpha_s r_2 a^2 \sum_{\mu,\nu} \text{Tr}(D_\mu F_{\nu\sigma} D_\mu F_{\nu\sigma}) \\ &+ \alpha_s r_3 a^2 \sum_{\mu,\nu} \text{Tr}(D_\mu F_{\mu\sigma} D_\nu F_{\nu\sigma}) \\ &+ \dots, \end{aligned} \quad (70)$$

that must be removed. The last term is harmless; its coefficient can be set to zero by a change of field variable (in the path integral) of the form

$$A_\mu \rightarrow A_\mu + a^2 \alpha_s f(\alpha_s) \sum_\nu D_\nu F_{\nu\mu}. \quad (71)$$

Since changing integration variables does not change the value of an integral, such field transformations must leave the physics unchanged.⁸ Operators that can be removed by a field transformation are called “redundant.” The other corrections are removed by renormalizing the coefficient of the rectangle operator $R_{\mu\nu}$ in the action, and by adding an additional operator. One choice for the extra operator is

$$C_{\mu\nu\sigma} \equiv \frac{1}{3} \text{Re} \text{Tr} \left[\text{Diagram} \right]. \quad (72)$$

⁸One must, of course, include the jacobian for the transformation in the transformed path integral. This contributes only in one-loop order and higher; it has no effect on tree-level calculations.

Then the action, correct up to $\mathcal{O}(a^2\alpha_s^2, a^4)$, is [15]

$$S = -\beta \sum_{x,\mu>\nu} \left\{ \frac{5}{3} \frac{P_{\mu\nu}}{u_0^4} - r_g \frac{R_{\mu\nu} + R_{\nu\mu}}{12 u_0^6} \right\} + c_g \beta \sum_{x,\mu>\nu>\sigma} \frac{C_{\mu\nu\sigma}}{u_0^6}, \quad (73)$$

where

$$r_g = 1 + .48 \alpha_s (\pi/a) \quad (74)$$

$$c_g = .055 \alpha_s (\pi/a). \quad (75)$$

The coefficients r_g and c_g are computed by “matching” physical quantities, like low-energy scattering amplitudes, computed using perturbation theory in the lattice theory with the analogous quantity in the continuum theory. The lattice result depends upon r_g and c_g ; these parameters are tuned until the lattice amplitude agrees with the continuum amplitude to the order in a and α_s required:

$$T_{\text{lat}}(r_g, c_g) = T_{\text{contin}}. \quad (76)$$

Note that tadpole improvement has a big effect on these coefficients. Without tadpole improvement, $r_g = 1 + 2\alpha_s$; that is, the coefficient of the radiative correction is four times larger. Tadpole improvement automatically supplies 75% of the one-loop contribution needed without improvement. Since $\alpha_s \approx 0.3$, the unimproved expansion for r_g is not particularly convergent. However, with tadpole improvement, the one-loop correction is only about 10–20% of r_g . Indeed, for most current applications, one-loop corrections to tadpole-improved actions are negligible.

Finally note that the twisted-rectangle action (66) must also be tadpole improved:

$$S_{\text{trt}} \equiv -\beta \sum_{x,\mu>\nu} \left\{ \frac{P_{\mu\nu}}{u_0^4} + \frac{T_{\mu\nu} + T_{\nu\mu}}{12 u_0^8} \right\}. \quad (77)$$

The correction term in this action has two more u_0 's than that in our other action. This makes S_{trt} much more dependent upon tadpole improvement. Comparing results generated by our two actions provides a sensitive test of tadpole improvement. The α_s corrections to this action have not yet been computed, but are probably unnecessary.

Exercise: Show that the gauge that maximizes $\langle 0 | \frac{1}{3} \text{Tr} U_\mu | 0 \rangle$ becomes Landau gauge ($\partial \cdot A = 0$) in the $a \rightarrow 0$ limit.

Exercise: Tadpole diagrams are only important because they are ultraviolet divergent; the loop integrations generate factors of $1/a^2$ that cancel the explicit a 's from the link operator U_μ . Consequently such contributions can be significantly reduced if the effective ultraviolet cutoff for the gluons is lowered. Lowering the cutoff by a factor of two, for example, would reduce tadpole contributions by a factor of four, rendering them harmless. This reduction is easily accomplished by smearing, where, for example,

$$A_\mu(x) \rightarrow \left(1 - \frac{\epsilon a^4 D^4}{n}\right)^n A_\mu(x). \quad (78)$$

The low-momentum components of the smeared A_μ field are identical, up to $\mathcal{O}(a^4)$ corrections, with the unsmeared field; but at high momentum the smearing factor acts as an ultraviolet cutoff

$$\left(1 - \frac{\epsilon a^4 D^4}{n}\right)^n \rightarrow \left(1 - \frac{\epsilon a^4 p^4}{n}\right)^n \approx e^{-\epsilon p^4 a^4}. \quad (79)$$

Tadpole improvement should be unnecessary when the smeared field is used in quark actions, etc., in place of the original field. Parameter ϵ is chosen to give the appropriate cutoff, while n is chosen sufficiently large that smearing factor approximately exponentiates as indicated. Design and test an implementation of this smearing scheme for the link variables U_μ .

Exercise: Lattice ϕ^4 theory has a^2 corrections of the form

$$\delta\mathcal{L} = c_1 a^2 \sum_\mu (\partial_\mu^2 \phi)^2 + c_2 a^2 \phi^6 + c_3 a^2 (\partial^2 \phi)^2 + c_4 a^2 \phi^3 \partial^2 \phi. \quad (80)$$

Find a field transformation

$$\phi \rightarrow \tilde{\phi} = \phi + a^2 f(\phi, \partial_\mu^2 \phi \dots) \quad (81)$$

that removes the c_3 and c_4 terms (that is, the redundant operators).

Note that $\phi \rightarrow \phi + \delta\phi$ implies

$$S[\phi] \rightarrow S + \delta\phi \frac{\delta S}{\delta\phi}. \quad (82)$$

Thus the leading redundant operators can be rearranged so that they are proportional to $\delta S/\delta\phi$. Since the classical field equation is $\delta S/\delta\phi = 0$, redundant operators are often said to have no effect “because of the equations of motion.” More precisely it is because they can be removed by a change of integration variable in the path integral.

Show that the jacobian $|\delta\phi/\delta\tilde{\phi}|$ has no effect at tree-level, but must be included when quantum loop corrections are important. (Hint: Try computing a simple scattering amplitude using perturbation theory in the original and in the transformed theory.)

3.3 Tests of the Gluon Action

Having a procedure for systematically improving the gluon action, we need to establish whether the improvements really do improve simulations.

The effects of the $\mathcal{O}(a^2)$ improvements in the gluon action are immediately apparent if one compares the static-quark potential computed, using (64), with the Wilson action (54) and with the improved action (73) [14]. Monte Carlo simulation results for these potentials are plotted in Fig. 4, together with the continuum potential. The Wilson action has errors as large as 40%. These are reduced to only 4–5% when the improved action is used instead.

The dominant errors in the uncorrected simulation of $V(r)$ reflect a failure of rotational invariance, which is expected since the a^2 error in the Wilson action (54) is neither Lorentz nor rotationally invariant. The points at $r = a, 2a, 3a \dots$ are for separations that are parallel to an axis of the lattice, while the points at $r = \sqrt{2}a, \sqrt{3}a \dots$ are for diagonal separations between the static quark and antiquark. In Table 1, I tabulate the error ΔV in the potential at $r = \sqrt{3}a$ for a variety gluon actions, with and without tadpole improvement and one-loop radiative corrections. As expected, the correction term in the action is significantly underestimated without tadpole improvement. The tadpole-improved action is very accurate both with and without one-loop corrections, suggesting that $\mathcal{O}(a^2\alpha_s)$ corrections are comparable to those of $\mathcal{O}(a^4)$ and therefore unimportant for most current applications.

I also include in Table 1 results obtained using the twisted-rectangle action S_{trt} in (77). This action gives a potential that is essentially identical to that obtained with the other improved action. The a^4 errors are very different in the two actions; their agreement suggests that a^4 errors are small. It also is striking confirmation of the importance of tadpole improvement since the u_0 's more than double the size of the correction term in the twisted-rectangle action when $a = 0.4$ fm.

Another test of our improved action is to compute physical quantities on lattices with several different lattice spacings, looking for evidence of finite- a errors. These are consistently small. For example, the temperature at which gluonic QCD has a deconfining phase transition can be computed using the improved the action. One finds [16]:

$$T_c = \begin{cases} 298 (6) \text{ MeV} & \text{for } a = .32 \text{ fm} \\ 309(6) (6) \text{ MeV} & \text{for } a = .21 \text{ fm.} \\ 303 (8) \text{ MeV} & \text{for } a = .16 \text{ fm.} \end{cases} \quad (83)$$

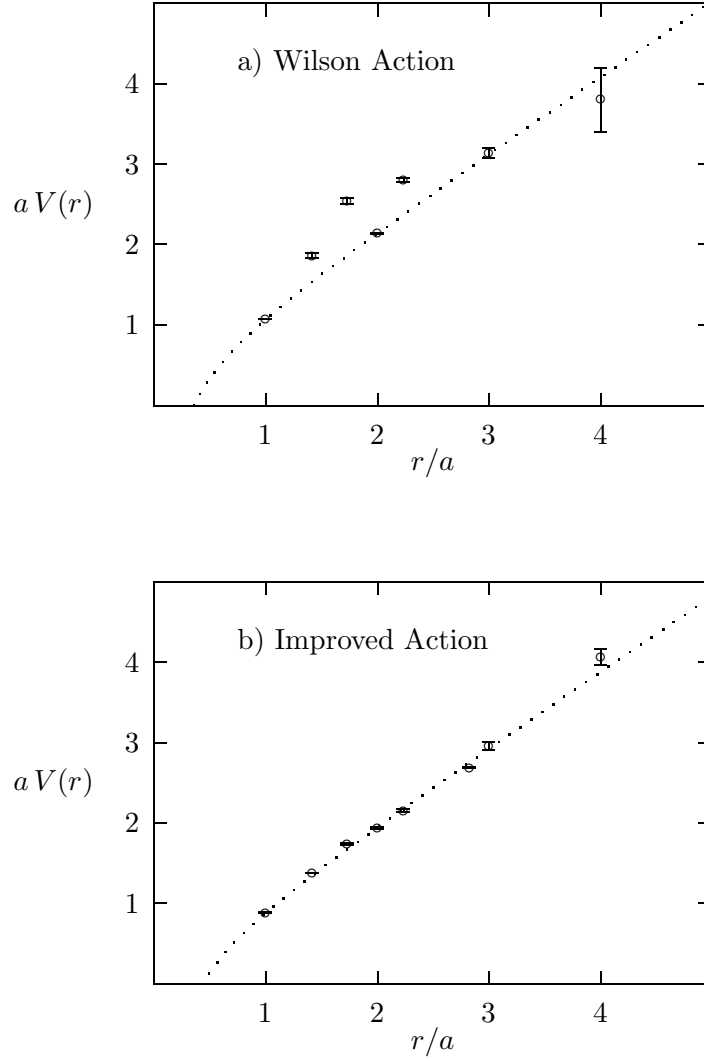


Figure 4: Static-quark potential computed on 6^4 lattices with $a \approx 0.4$ fm using the Wilson action and the improved action. The dotted line is the standard infrared parameterization for the continuum potential, $V(r) = Kr - \pi/12r + c$, adjusted to fit the on-axis values of the potential.

Table 1: Error in the static quark potential at $V(\sqrt{3}a)$ for a variety of gluon actions. The lattice spacing in each case is $a \approx .4$ fm; K is the slope of the linear part of the static potential.

Action	$\Delta V(\sqrt{3}a)/K\sqrt{3}a$
unimproved (Wilson)	.41 (2)
tree-level improved, no tadpole improvement	.15 (1)
one-loop improved, no tadpole improvement	.12 (2)
tree-level improved, with tadpole improvement	.05 (1)
one-loop improved, with tadpole improvement	.04 (1)
twisted-rectangle correction, with tadpole improvement	.04 (2)

The results all agree to within statistical errors of a few percent.

3.4 Anisotropic Lattices and Tuned Gluon Actions⁹

As a final illustration of improved gluon actions with tadpole-improved operators, I now show results of simulations employing anisotropic lattices with temporal lattice spacings a_t that are smaller than the spatial lattice spacings a_s . Such anisotropic lattices lead to greatly improved signal-to-noise in Monte Carlo simulations of hadrons; they are also useful for designing improved quark actions, as I discuss later. On an anisotropic lattice, our rectangle-improved action becomes

$$\begin{aligned}
 S = & -\beta \sum_{x, s > s'} \frac{a_t}{a_s} \left\{ \frac{5}{3} \frac{P_{ss'}}{u_s^4} - \frac{1}{12} \frac{R_{ss'}}{u_s^6} - \frac{1}{12} \frac{R_{s's}}{u_s^6} \right\} \\
 & -\beta \sum_{x, s} \frac{a_s}{a_t} \left\{ \frac{5}{3} \frac{P_{st}}{u_s^2 u_t^2} - \frac{1}{12} \frac{R_{st}}{u_s^4 u_t^2} - \frac{1}{12} \frac{R_{ts}}{u_t^4 u_s^2} \right\},
 \end{aligned} \tag{84}$$

where s and s' are spatial directions. The mean links u_t and u_s are different on anisotropic lattices. When $a_t \leq a_s/2$, u_t is very close to its continuum

⁹This section is based on work with M. Alford, T. Klassen, C. Morningstar, M. Peardon and H. Trottier.

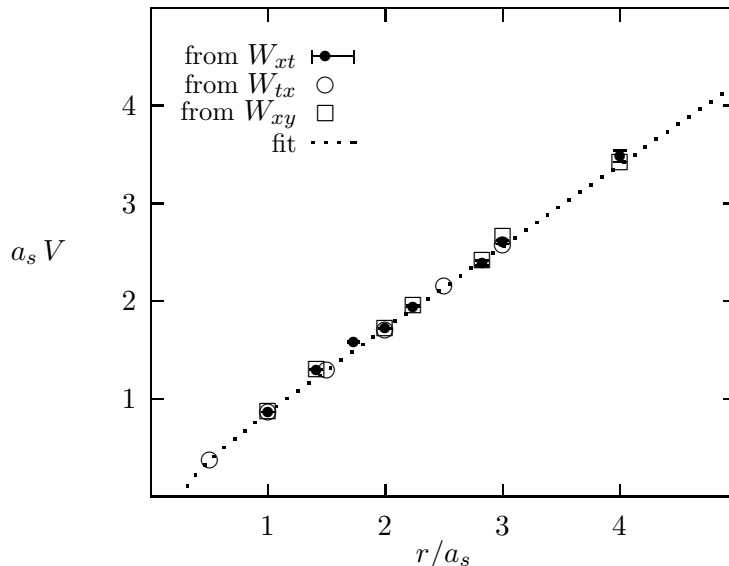


Figure 5: The static-quark potential computed on an anisotropic lattice in different orientations. Results are shown for a_t/a_s equal 1/2. Except as shown, analysis errors are smaller than the plot symbols. The fit in each plot is to the open circles; the fitting function is $V(r) = Kr - b/r + c$.

value of one. Thus we take

$$u_t = 1 \quad (85)$$

$$u_s = \langle P_{ss'} \rangle^{1/4}. \quad (86)$$

The same u_s , to within a few percent, can be obtained from the link expectation value in Coulomb gauge, which is the natural gauge choice for anisotropic lattices with small a_t 's.

The anisotropic simulation can be tested by comparing the static quark potential computed from Wilson loops in different orientations: loops in the $x-t$ plane, loops in the $x-y$ plane, and loops in the $t-x$ plane (with x playing the role of time). If the anisotropic theory is tadpole-improved all three potentials agree (Fig. 5). Without tadpole-improvement the slopes disagree by 20% (Fig. 6).

The coefficients of the correction terms in the gluon action for anisotropic

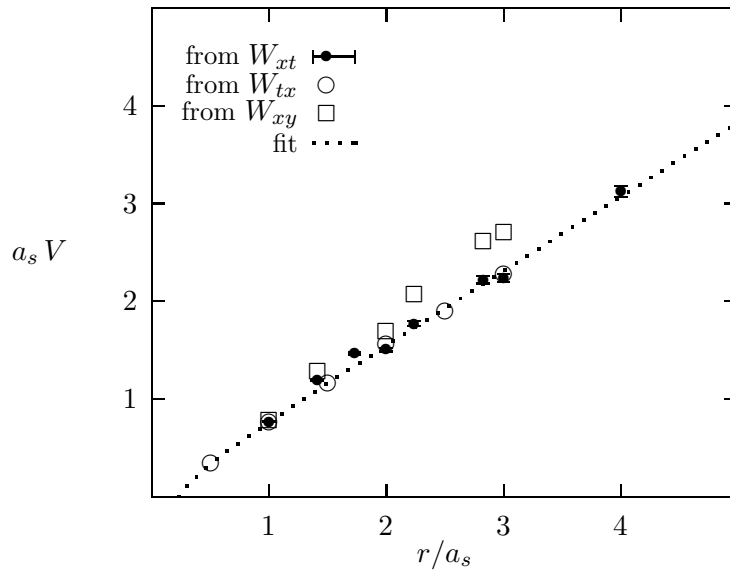


Figure 6: The static-quark potential computed on an anisotropic lattice in different orientations, as in the previous figure. The action used here was not tadpole improved. The input value for a_t/a_s is $1/2$.

lattices are known only to leading order in α_s . While it is clear from the simulations that tadpole improvement captures the bulk of the renormalizations, these same simulations provide a handle on further radiative corrections. This is because the leading corrections in the gluon action affect the extent to which continuum symmetries, like rotation invariance, are restored. We can use symmetry restoration as a criterion for tuning the couplings beyond their tadpole-improved tree-level values. Thus, for example, the static potential at $\mathbf{r} = (a_s, 2a_s, 2a_s)$ should agree exactly with that at $\mathbf{r} = (3a_s, 0, 0)$. One might tune the value of the spatial mean link u_s used in the action until this is the case. Similarly one would like the anisotropy a_t/a_s built into the action to agree with the renormalized anisotropy coming out of the simulations. The ratio u_t/u_s can easily be tuned to make the two agree exactly. Such tuning does not capture all of the $\mathcal{O}(\alpha_s)$ corrections except in the simplest of situations. However it may be a useful intermediate step between tree-level tadpole improvement and a full perturbative analysis of the radiative corrections.

Exercise: One defect of our improved gluon action is that the gluon spectrum has ghosts. These are caused by the R_{ts} terms in the action, which extend two steps in the time direction. (Numerical ghosts, like these, are discussed in greater detail in the section on light quarks.) These gluon ghosts, being at high energies (of order $2.6/a_t$), should have little effect on simulation results, particularly for smaller a_t 's; this is confirmed by simulations. Nevertheless one might wish to remove them completely. This is easily done, when a_t is small compared with a_s , by dropping the R_{ts} terms in the action. This introduces new errors of order a_t^2 but these will be negligible relative to the a_s^4 errors provided a_t is small enough. Modify the st terms in the action so that all a_s^2 errors are still canceled in the absence of the R_{ts} contribution.

3.5 Summary

In this section I have outlined how one designs actions for simulating gluon dynamics on coarse lattices. The simulation results show that accurate simulations are possible even on lattices as coarse as $a = .4$ fm using very simple actions. Tadpole improvement is essential, but one-loop radiative corrections to the action are not too important. Rotational invariance of the potential and, for anisotropic lattices, space-time interchange symmetry provide sensitive tests of improved gluon actions, and can be used to tune the leading correction terms.

The coarse lattices make simulations very fast. Most of the simulation results shown here were obtained using an IBM RS6000/250 desktop work-

station, which is powered by a personal-computer CPU (66MHz PowerPC). Any of these results could be generated easily on a high-end personal computer.

4 Light Quarks on Coarse Lattices¹⁰

In this section I develop techniques for designing very accurate discretizations of the Dirac equation for quarks in a gluonic field. I begin by reviewing various resolutions of the “doubling problem” which plagues even the simplest discretization. I then discuss two currently popular discretizations, and finally new discretizations that are significantly more accurate.

4.1 Naive Discretization and Doubling

The euclidean Dirac lagrangian in the continuum is

$$\mathcal{L} = \bar{\psi} (\mathbf{D} \cdot \boldsymbol{\gamma} + m) \psi \quad (87)$$

where

$$\{\gamma_\mu, \gamma_\nu\} = 2 \delta_{\mu\nu} \quad (88)$$

and I take

$$\gamma_t = \begin{pmatrix} 1 & 0 \\ 0 & -1 \end{pmatrix} \quad \gamma_s = \begin{pmatrix} 0 & \sigma_s \\ \sigma_s & 0 \end{pmatrix} \quad \gamma_5 \equiv \gamma_t \gamma_x \gamma_y \gamma_z = i \begin{pmatrix} 0 & 1 \\ -1 & 0 \end{pmatrix} \quad (89)$$

where, again, s and t as subscripts signify spatial and temporal indices respectively. The obvious discretization is

$$\mathcal{L}_{\text{lat}} = \bar{\psi} \left(\Delta \cdot \boldsymbol{\gamma} + m + \mathcal{O}(a^2) \right) \psi \quad (90)$$

where now Δ_μ is a (tadpole-improved) gauge-covariant derivative:

$$\Delta_\mu \psi(x) \equiv \frac{U_\mu(x) \psi(x + a\hat{\mu}) - U_\mu^\dagger(x - a\hat{\mu}) \psi(x - a\hat{\mu})}{2 a u_0}. \quad (91)$$

The other finite-difference operators, $\Delta_\mu^{(2)}$, $\Delta_\mu^{(3)}$. . . , can all be made gauge-covariant by adding U_μ 's as in Δ_μ ; in what follows I will always use these symbols to refer to the gauge-covariant differences.

¹⁰This section is based on work with M. Alford and T. Klassen.

Unfortunately this simple lattice Dirac action has a very serious pathology. To see this consider the $\mathbf{p} = 0$ spin-up solution of the corresponding Dirac equation without gluon fields:

$$\psi_{\uparrow}(t) = e^{-Et} \begin{bmatrix} 1 \\ 0 \\ 0 \\ 0 \end{bmatrix} \quad (92)$$

(There is no i in the exponent because t is euclidean; E is the minkowski energy.) Substituting into the Dirac equation,

$$(\Delta \cdot \gamma + m) \psi_{\uparrow}(t) = 0, \quad (93)$$

we obtain

$$(\Delta_t + m) e^{-Et} = 0 \quad \implies \quad \frac{e^{-aE} - e^{aE}}{2a} + m = 0. \quad (94)$$

This equation is quadratic in $z \equiv \exp(aE)$ and therefore it has two solutions for E . We only want one! The two solutions are

$$E = \begin{cases} m + \mathcal{O}(a^2) & \text{(normal)} \\ -m + i\pi/a + \mathcal{O}(a^2) & \text{(doubler)} \end{cases}. \quad (95)$$

The first is the solution we want; the second is known as a “doubler.”

The possibility of a second solution for the energy is obvious from inspection of the lattice Dirac equation. The problem lies in the $\Delta_t \psi$ term. This links ψ 's two lattice spacings apart which means that the dispersion relation is second order in $z \equiv \exp(aE)$. In general one expects n roots if the ψ 's are spread over n lattice spacings — a potential problem when we go to improve the discretization. The doubler cannot be ignored. It is related to the normal solution by a symmetry of the gluon-free lattice theory: if $\psi(\mathbf{x}, t)$ is a solution of the lattice Dirac equation then so is

$$\tilde{\psi}(\mathbf{x}, t) \equiv i\gamma_5 \gamma_t (-1)^{t/a} \psi(\mathbf{x}, t). \quad (96)$$

This symmetry operation turns the normal solution into the doubler solution. Consequently the doubler acts as an extra flavor of quark, which is degenerate with the normal quark (when there are no gauge fields). Furthermore, in euclidean space there is nothing unique about the time direction.

Thus there is an analogous doubling symmetry for each direction, and successive transformations involving two or more directions also are symmetries. This implies that there are fifteen doublers in all.

The root of the doubler problem lies in the finite-difference approximation for first-order derivatives. Fourier transforming ∂ and Δ we obtain

$$\partial \rightarrow \text{I}p \quad (97)$$

$$\Delta \rightarrow \text{I} \sin(pa)/a. \quad (98)$$

These agree well for low momenta, but, as p approaches the ultraviolet cutoff π/a , the transform of Δ vanishes rather than becoming large. As a consequence, for example, high-momentum states can have very low or even vanishing energies. This is disastrous. Note that the same problem does not arise for second-order derivatives:

$$\partial^2 \rightarrow -p^2 \quad (99)$$

$$\Delta^{(2)} \rightarrow -\left(\frac{2}{a} \sin(pa/2)\right)^2. \quad (100)$$

Although the transform of $\Delta^{(2)}$ becomes quite different from p^2 at large p , it nevertheless remains large, going to its maximum of $4/a^2$ at the ultraviolet cutoff. Second-order (and higher even-order) derivatives do not cause doubling problems.

I will discuss two approaches to the doubling problem. One involves adding operators to the quark action that are almost redundant but remove the doublers or drive them to high energies. The other involves “staggering” the quark degrees of freedom on the lattice.

Exercise: Show that gauge transformation

$$\psi(x) \rightarrow \Omega(x) \psi(x) \quad U_\mu(x) \rightarrow \Omega(x) U_\mu(x) \Omega(x + a\hat{\mu})^\dagger. \quad (101)$$

implies that

$$\Delta_\mu \psi(x) \rightarrow \Omega(x) \Delta_\mu \psi(x). \quad (102)$$

Also show that (setting $u_0=1$)

$$\Delta_\mu = \frac{e^{aD_\mu} - e^{-aD_\mu}}{2a}. \quad (103)$$

(Hint: Why can't there be $F_{\mu\nu}$'s on the right-hand side?) This relation is crucial to what follows; find a different definition of the the covariant difference operator Δ for which this relation is incorrect in $\mathcal{O}(a)$.

4.2 Field Transformations to Remove Doublers

The first approach to removing the doublers is to introduce into the action an operator that is redundant up to $\mathcal{O}(a^2)$ and has higher order non-redundant parts that drive the doubler to high energies. A redundant operator remember, is one that can be eliminated from the action by a change of variables on the quark fields in the path integral, and hence has no effect on any physical observables. For example, consider the field transformation from the continuum field ψ_c to a new field ψ where

$$\begin{aligned}\psi_c &= \left[1 - \frac{ra}{4} (\Delta \cdot \gamma - m_c) \right] \psi \\ &\equiv \Omega \psi,\end{aligned}\tag{104}$$

and

$$\bar{\psi}_c = \bar{\psi} \Omega\tag{105}$$

With this transformation our naive lattice action becomes

$$\bar{\psi}_c (\Delta \cdot \gamma + m_c) \psi_c = \bar{\psi} \Omega (\Delta \cdot \gamma + m_c) \Omega \psi\tag{106}$$

$$= \bar{\psi} \left[\Delta \cdot \gamma + m - \frac{ra}{2} \left(\Delta \cdot \Delta + \frac{\sigma \cdot gF}{2} \right) \right] \psi + \mathcal{O}(a^2)\tag{107}$$

where $m \equiv m_c + ram_c^2/2$. In deriving the final formula we used the lattice version of the identity

$$(\mathbf{D} \cdot \gamma)^2 = \mathbf{D} \cdot \mathbf{D} + \frac{\sigma \cdot gF}{2}\tag{108}$$

where

$$\sigma_{\mu\nu} \equiv -\frac{i}{2} [\gamma_\mu, \gamma_\nu].\tag{109}$$

The new $\mathcal{O}(a)$ term in the transformed lagrangian does not introduce new $\mathcal{O}(a)$ errors because it results from a field transformation; it is redundant in the sense discussed above for gluon operators. In its present form this term also has no effect on the doubling problem. The trick is to replace the operator $\Delta \cdot \Delta$, which vanishes at the ultraviolet cutoff, with $\Delta^{(2)}$, which is the same up to $\mathcal{O}(a^2)$ errors in the infrared but large at the ultraviolet cutoff. The $\Delta^{(2)}$ pushes the doublers off to high energies, of order $1/a$, where they are harmless. Thus an $\mathcal{O}(a)$ -accurate quark action that is doubler free is

$$\mathcal{L}_{\text{SW}} = \bar{\psi} \left[\Delta \cdot \gamma + m - \frac{ra}{2} \left(\Delta^{(2)} + \frac{\sigma \cdot gF}{2} \right) \right] \psi\tag{110}$$

$$= \bar{\psi}_c (\mathbf{D} \cdot \gamma + m_c) \psi_c + \mathcal{O}(a^2),\tag{111}$$

where, again,

$$\psi_c = \Omega \psi \quad m = m_c + ram_c^2/2. \quad (112)$$

This is the Sheikholeslami-Wohlert (SW) quark action [17]. It becomes Wilson's original action if the $\sigma \cdot gF$ term is dropped (resulting in $\mathcal{O}(a^1)$ errors).

We can check that the doublers are removed by again substituting the $\mathbf{p}=0$ solution into the corresponding Dirac equation. We obtain

$$\begin{aligned} \left(\Delta_t + m - \frac{ra}{2} \Delta^{(2)} \right) e^{-Et} &= 0 \\ \implies (1-r)e^{-aE} - (1+r)e^{aE} + 2r + 2am &= 0. \end{aligned} \quad (113)$$

which has roots

$$E = \begin{cases} m_c + \mathcal{O}(a^2) & \text{(normal)} \\ (1/a) \ln [(r-1)/(r+1)] + \dots & \text{(ghost)} \end{cases}. \quad (114)$$

The doubler has been replaced by a high-energy ‘‘ghost’’ particle, as desired. The ghost goes away completely for $r=1$.

Exercise: Create a lattice version of $F_{\mu\nu}$ for use in the SW quark action. Build your operator out of tadpole-improved link operators. Try designing a discretization that is accurate up to corrections of $\mathcal{O}(a^4)$.

4.3 a^3 -Accurate Lattice Dirac Theory

Our numerical experiments in the first Section suggest that the a^2 errors in the SW quark action might still be quite large when the lattice spacing is of order .4 fm. Thus it is worthwhile developing a quark action that has errors only of order a^4 and higher.

A attempt at such an improved Dirac theory is the action

$$\bar{\psi} \left[\Delta \cdot \gamma - \frac{a^2}{6} \Delta^{(3)} \cdot \gamma + m_c \right] \psi \quad (115)$$

where the a^2 correction cancels the leading errors induced by the $\Delta \cdot \gamma$ term. Not surprisingly this action is plagued with doublers and ghosts. Since the temporal derivatives extend two steps in each direction, the energy dispersion relation has four branches instead of one.

There are several approaches one can take to solving this doubler disaster. The ‘‘D234’’ quark actions rely upon three ingredients [18]:

1. anisotropic lattices, with $a_t \leq a_s/2$, which push ghost states to higher energies, where they decouple. This works because ghost energies are governed by the temporal lattice spacing and grow like $1/a_t$ when a_t is reduced. Reducing the temporal lattice spacing also makes Monte Carlo measurements of hadron propagators much more efficient.
2. redundant operators like

$$-\frac{r a_t}{2} \left(\Delta^{(2)} + \frac{\sigma \cdot gF}{2} + \dots \right) \quad (116)$$

in the quark action, which can be tuned to remove some of the doublers and ghosts.

3. “irrelevant” operators like

$$s a_t^3 \Delta_t^{(4)} \quad (117)$$

in the quark action, which have negligible effect on low-momentum physics (if $a_t \leq a_s/2$) but are useful at high energies for removing doublers and ghosts. Terms involving higher-order spatial derivatives, like $a_s^4 \Delta_s^{(6)}$, can also be added.

A variety of actions can be created by combining differing amounts of redundant and irrelevant operators. In general one tries to tune these additions to minimize the number and importance of ghost states, to give the best low-momentum behavior, and to minimize pathologies at high momentum.

A simple example of a D234-type action is obtained by generalizing our derivation of the SW action. We begin with a field transformation $\psi_c \rightarrow \psi$ where

$$\psi_c = \Omega \psi \quad (118)$$

with

$$\Omega \equiv 1 - X - \frac{X^2}{2} - \frac{X^3}{2} \quad (119)$$

$$= \sqrt{1 - 2X} + \mathcal{O}(X^4) \quad (120)$$

and

$$X \equiv \frac{r a_t}{4} \left(\Delta \cdot \gamma - \sum_{\mu} \frac{a_{\mu}^2}{6} \Delta_{\mu}^{(3)} \gamma_{\mu} - m_c \right) \quad (121)$$

$$= \frac{r a_t}{4} \left(D \cdot \gamma - m_c + \mathcal{O}(a^4) \right). \quad (122)$$

Applying this transformation to the naive improved action (115) and adding an irrelevant a_t^3 operator, we obtain¹¹

$$\begin{aligned} \mathcal{L}_{\text{D234x}} = & \bar{\psi} \left[\Delta \cdot \gamma - \sum_{\mu} \frac{a_{\mu}^2}{6} \Delta_{\mu}^{(3)} \gamma_{\mu} + m \right. \\ & - \frac{r a_t}{2} \left(\Delta^{(2)} - \sum_{\mu} \frac{a_{\mu}^2}{12} \Delta_{\mu}^{(4)} + \frac{\sigma \cdot gF}{2} \right) \\ & \left. + s a_t^3 \Delta_t^{(4)} \right] \psi. \end{aligned} \quad (123)$$

This action is the same as the continuum action up to corrections of order a_t^3 and a_s^4 . It is easy to show that the choice

$$s = \frac{1}{12} - \frac{r}{24} \quad (124)$$

removes one of the ghost/doubler states, leaving two ghosts that have high energies for any value of r near 1. If in addition $r = 2/3$ is chosen, a second ghost disappears and only one remains (with an energy of order $2/a_t$.) The free-quark dispersion relation for this set of parameters is shown in Fig. 7 for a lattice with $a_s = 2 a_t = .4 \text{ fm}$; the ghost is roughly 2 GeV above the real quark and so harmless in most applications.

4.4 Tests of Quark Action

Highly improved actions like the D234x action (123) have a large number of bare coupling constants that must be computed in perturbation theory — one for each term in the action. In the previous section we worked only to lowest order (tree-level) in perturbation theory. However our discussion of the gluon action suggests that this is sufficiently accurate provided all operators are tadpole improved; the renormalizations due to $k > \pi/a$ physics affect physical quantities by only a few percent. How can we ascertain whether the same is true of our quark actions?

¹¹The designers of this action, having examined a large number of similar actions, all very effective, are currently grappling with a nomenclature crisis. I refer to the particular action shown here as the “D234x” action, but this is certainly not its final name. Most of what I say about this action is true of almost all other D234 actions, and so “D234x” can usually be taken to refer to a generic D234 action.

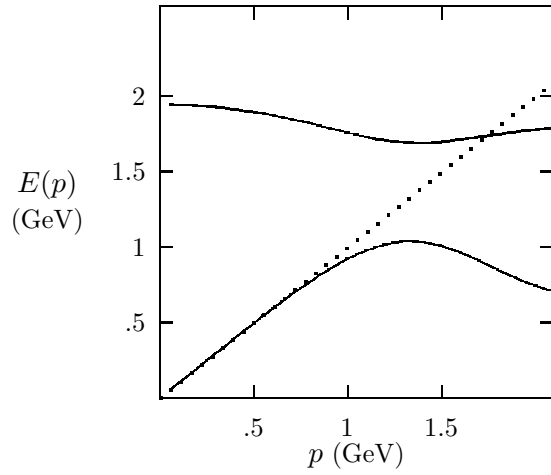


Figure 7: Dispersion relation for a free massless lattice quarks described by the D234x action. A low-energy, physical branch and a high-energy ghost branch are shown, together with the continuum dispersion relation (dotted line). Energies are for momenta proportional to $(1, 1, 0)$.

One powerful approach is to verify that continuum symmetries are restored by the corrections. For example, the leading error in the discretized Dirac operator, $\Delta \cdot \gamma + m$, breaks Lorentz invariance. The $a_\mu^2 \Delta_\mu^{(3)} \gamma_\mu$ term in the D234x action is meant to cancel this error. We can check that this term has done its job by comparing the dispersion relation of a meson (or baryon) computed in a simulation with the Lorentz-invariant dispersion relation of the continuum. In a Lorentz-invariant theory, a hadron's energy $E_h(\mathbf{p})$ and its three momentum \mathbf{p} are such that the combination

$$c^2(\mathbf{p}) \equiv \frac{E_h^2(\mathbf{p}) - m_h^2}{\mathbf{p}^2} \quad (125)$$

is independent of \mathbf{p} and equal to the square of the speed of light ($=1$). In Fig. 8 I show D234x simulation results for meson's $c(\mathbf{p})$. The lattice for this simulation is very coarse, with $a_s = 2a_t = .4$ fm, and yet $c(\mathbf{p})$ is within a few percent of one all the way out to momenta of order 1 GeV ($\approx 2/a_s$). For comparison I include the same quantity calculated using the SW action (on an isotropic lattice), which has no correction for the a^2 error; it has 25% errors by $p=1$ GeV, and the momentum dependence of the discrepancy is consistent with the quadratic errors expected. This comparison shows that the coefficient of the a^2 correction in the D234x action is not renormalized by more than 10–20%, and that this renormalization will have no more than a few percent effect on low-momentum physics. The momenta used for the Monte Carlo points shown in this plot include momenta that are parallel to a lattice axis, and momenta that point along lattice diagonals; the fact that different momenta agree to within a few percent shows that rotation invariance is also restored by the correction term.

The $c(\mathbf{p})$ plot provides a second important check on the D234x action. On anisotropic lattices, the symmetry between space and time is not exact. Consequently the spatial and temporal parts of the leading Dirac operator $\Delta \cdot \gamma$ are renormalized differently:

$$D \cdot \gamma \rightarrow \Delta_t \gamma_t + c_0 \mathbf{\Delta} \cdot \boldsymbol{\gamma}, \quad (126)$$

where c_0 is a bare speed-of-light,

$$c_0 = 1 + \text{const } \alpha_s + \dots \quad (127)$$

Such a renormalization would shift the low-momentum values of $c(\mathbf{p})$ away from one. In fact, with only our tree-level action, $c(\mathbf{p}) = 1.025(20)$ at

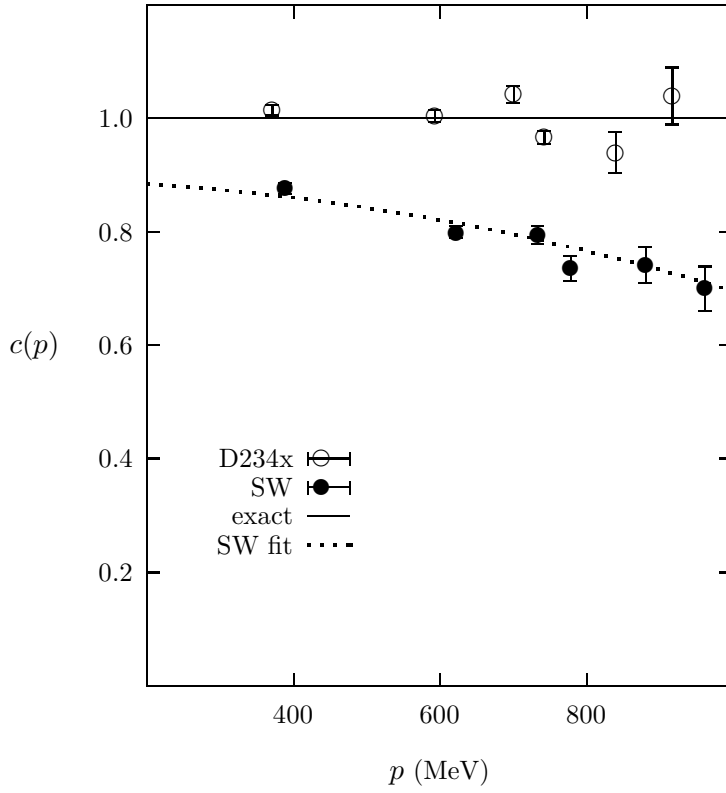


Figure 8: The speed of light computed using the D234x and SW quark actions from the energy and three momenta of a meson. The fit to the SW data is $\tilde{c}_0 + k(ap)^2$ where \tilde{c}_0 and k are constants.

Table 2: Mass differences between two simulations, one with $r=1$ and the other with $r=2/3$, for different quark masses. The bare quark masses in the two simulations were tuned to give the same m_π/m_ρ .

m_π/m_ρ	Δm_π	Δm_ρ	Δm_N	Δm_Δ
.65	0.6 (2) %	-0.13 (13) %	-0.3 (2) %	0.4 (3) %
.57	0.6 (4) %	-0.6 (1.0) %		

low momenta; parameter c_0 must be within a percent of one. Note that this success depends crucially on tadpole improvement; without tadpole improvement $c(\mathbf{p}) = 1.2$ at low momenta on our $a_s = .4$ fm lattice.

The only other potentially large renormalization is in the $\mathcal{O}(r a_t)$ terms induced by the field transformation. Again there is a symmetry associated with this term: field-redefinition or “ r symmetry”. The operator multiplied by r is redundant and so should have no effect on the low-momentum physics. Consequently the low-momentum physics should be invariant under changes in the value of r . If the renormalizations of the $\Delta^{(2)}$ and $\sigma \cdot gF$ terms in the action are very different, then the tree-level operator is no longer redundant and results must change as r is varied; on the other hand, if the renormalizations are roughly the same then the net effect of the renormalizations is a harmless shift in r .¹² The results of such an r -test for a close relative of the D234x action are shown in Table 2. These show that the pion, rho, nucleon and delta masses all shift by less than a percent when r is changed from 2/3 to 1. Since omitting the $\sigma \cdot gF$ term shifts masses by 20%, our r -test implies that the relative renormalization given by tree-level tadpole improvement is correct to within roughly 10–20%. A 10% change in the coefficient of $\sigma \cdot gF$ would shift the meson masses by only 2%.

In [19] a different test of the $\sigma \cdot gF$ coefficient is proposed. This is based on the fact that the r terms in the action break the quark’s chiral symmetry even for massless quarks. If the $\sigma \cdot gF$ coefficient is properly tuned, the chiral symmetry breaking terms are redundant and the chiral symmetry Ward identity should be restored. Using Monte Carlo evaluations of the various terms involved, the authors tune the coefficient until the identity

¹²I am simplifying the discussion here. On an anisotropic lattice, where space–time interchange is not an exact symmetry, the temporal and spatial parts of $\Delta^{(2)}$ and $\sigma \cdot gF$ have different radiative corrections. Thus the r -test is checking on the relative coefficients of four operators, as opposed to two in the isotropic case.

is satisfied. Working only with the SW action and relatively small lattice spacings, they find renormalizations that are larger than those above for D234: the coefficient of $\sigma \cdot gF$ in the SW action is a little more 20% larger than the tadpole-improved tree-level coefficient at $a \approx .1$ fm. Such a shift at such small lattice spacings has only a small effect on hadron masses; but in the same study the authors encountered pathological behavior in the SW action, with this correction, at large lattice spacings. Also the correction to tadpole improvement, though small throughout the range of their study, grows much more rapidly than naively expected as a increases from .03 fm to .1 fm. It would be very interesting to verify these results using the r -test, which provides an independent method of testing the same correction.

Our tests of the D234 action confirm that tree-level improvement of the quark action, using tadpole-improved operators, is quite accurate. However the work I just described concerning the SW action suggests that nonperturbative tuning of parameters in the action may be important for some actions and operators. Such tuning is straightforward for D234: the same tests I described above can be used to tune the leading corrections in the action. In particular, the c_0 parameter, which is potentially the most important, can be easily adjusted so that $c(\mathbf{p}=0) = 1$.

Finally, in Fig. 9, I show simulation results for the rho mass as a function of lattice spacing. I give results for the D234x action [18], which should have a_s^4 errors, for the SW action [20], which should have a^2 errors, and for the Wilson action [21], which should have a^1 errors. The D234x and SW simulations use an improved gluon action; the Wilson results are for an uncorrected gluon action. Assuming that the a dependence of the errors is as expected, all three actions agree quite well on the continuum limit ($a \rightarrow 0$) mass of the rho, but the more improved the quark action, the sooner it gets there. This figure demonstrates very clearly that we know how to systematically improve quark actions for use on very coarse lattices. Furthermore it is clear that simulations that are accurate to within a few percent are possible on lattices with spatial lattice spacings between .3 and .4 fm.

4.5 t -Staggered Quarks

A second approach to removing doublers is to “stagger” the quark degrees of freedom on the lattice. If we rewrite the Dirac field in terms of two

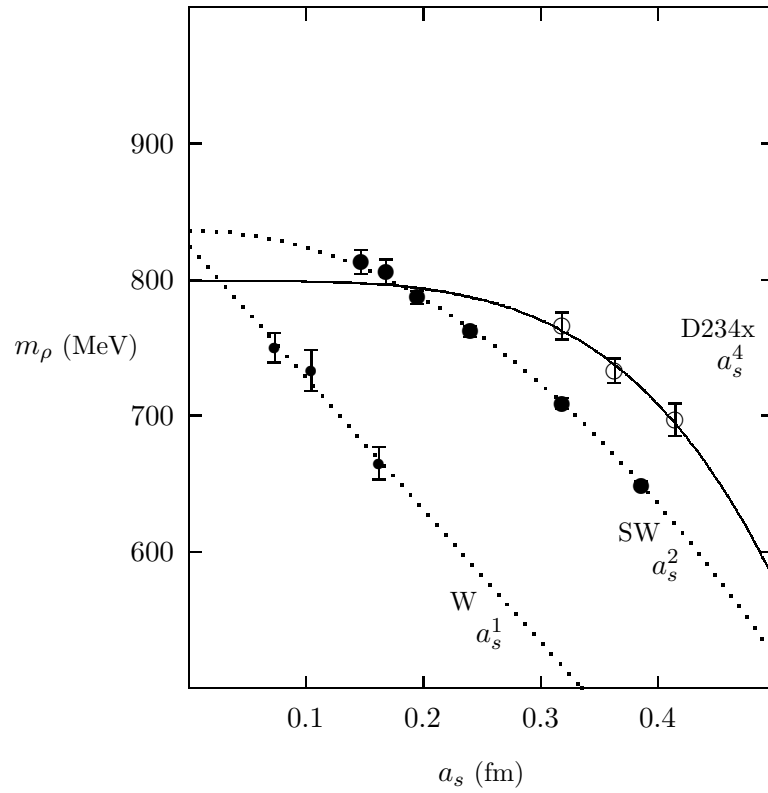


Figure 9: Rho mass versus lattice spacing computed using the Wilson quark action (W), the Sheikholeslami-Wohlert action (SW) and the D234x action. The charmonium S-P splitting was used to determine a_s . These simulations have no quark vacuum polarization and therefore the rho mass is expected to differ from its experimental value.

two-component fields, ϕ and χ ,

$$\psi = (\gamma_t)^{t/a_t} \begin{bmatrix} \phi + \chi \\ \phi - \chi \end{bmatrix} \quad (128)$$

the naive lattice Dirac equation (90) falls apart into two decoupled two-component equations:

$$\left(m_c + \Delta_t + (-1)^{t/a_t} \mathbf{\Delta} \cdot \boldsymbol{\sigma} \right) \phi = 0 \quad (129)$$

$$\left(m_c + \Delta_t + (-1)^{1+t/a_t} \mathbf{\Delta} \cdot \boldsymbol{\sigma} \right) \chi = 0 \quad (130)$$

The second equation is identical to the first equation, but shifted one lattice spacing in the t direction; it leads to identical quark physics. One of these equations describes the quark while the other describes the degenerate doubler. We get rid of the (temporal) doubler simply by dropping one of the two equations, say the second one. The remaining equation describes two quark polarizations and two antiquark polarizations, but no doublers. This approach is called “staggered” because dropping the χ field is equivalent to specifying only half the spinor components of the original Dirac field on time slices of the lattice with even t/a_t , while only the other half are specified on time slices with odd t/a_t . The spinor components are staggered between time slices.

This discretization still has a^2 errors and the spatial derivatives have poor behavior at high momentum. These problems are easily remedied by replacing

$$\mathbf{\Delta} \rightarrow \mathbf{\Delta} - \frac{a_s^2}{6} \mathbf{\Delta}^{(3)} \quad (131)$$

$$m \rightarrow m - s a_s^5 \left(\mathbf{\Delta}^{(2)} \right)^3 \quad (132)$$

in (129), where the correction terms involve spatial derivatives only. The parameter s is set at some small value ($\approx .02$) that is large enough to keep the high-momentum energy large but small enough that it has little effect on the low-momentum physics. The corrected equations still have a_t^2 errors, but these are negligible on anisotropic lattices with $a_t \leq a_s/2$.

This action has never been tried. It should be as accurate as the D234-type actions. It has half as many fields, no field transformation, no ghosts, and is somewhat simpler than the D234 actions; it may well be competitive.

A more conventional action, the Kogut-Susskind or staggered-quark action, is obtained by staggering the quark degrees of freedom in spatial as

well as temporal directions. This reduces the number of doublers to only three (from fifteen in the original naive action). Rather than removing the remaining doublers, in this approach one treats them as three extra flavors of quark. If these extra flavors were degenerate with the original quark, this approach might be computationally very efficient, perhaps giving four times the statistics for the same computational cost as other discretizations. Unfortunately the gluonic interactions lift the degeneracy between the flavors in the simplest version of this theory, resulting in significant mass differences. It would be very interesting to develop improved versions of this theory where the degeneracy is more accurately preserved.

4.6 Summary

Temporal derivatives usually cause problems when improving the discretization of an action. This is because successive improvements to the temporal derivatives involve operators that are increasingly nonlocal in time and therefore that almost inevitably result in ghosts of one sort or another. This problem is unusually serious for quark actions where even the leading-order discretization leads to doublers.

As illustrated in the previous sections, there are two standard techniques for removing the doublers. One is to introduce redundant operators that break the doubling symmetry; this leads to the SW and D234-type actions. The second is to stagger the quark spinor components on the lattice; this leads to actions for t -staggered quarks and Kogut-Susskind quarks.

Having repaired the leading-order operator, we face an even more acute problem in the a_t^2 correction to $\Delta_t \gamma_t$. This can be dealt with, as in the D234 actions, by using anisotropic lattices, with reduced a_t 's, to push the ghosts to high energies, and by adding irrelevant operators to cancel some of the ghosts. Alternatively, using anisotropic lattices, one might leave the a_t^2 errors uncorrected; these will be negligible compared with a_s^4 errors provided a_t is small enough compared with a_s . (Numerical experiments suggest that the a_t^2 errors are only a few percent when a_t is less than .2 fm.) A more complicated alternative, which I have not discussed, is to add irrelevant operators that replace the $a_t^2 \Delta_t^{(3)} \gamma_t$ correction term with less troublesome operators: for example, one can replace

$$\Delta_t^{(3)} \gamma_t \quad \rightarrow \quad -\frac{1}{2} \left[(\boldsymbol{\Delta} \cdot \boldsymbol{\gamma} + m_c) (\Delta_t \gamma_t)^2 + (\Delta_t \gamma_t)^2 (\boldsymbol{\Delta} \cdot \boldsymbol{\gamma} + m_c) \right] \quad (133)$$

$$\quad \rightarrow \quad (\boldsymbol{\Delta} \cdot \boldsymbol{\gamma} + m_c) \Delta_t \gamma_t (\boldsymbol{\Delta} \cdot \boldsymbol{\gamma} + m_c) \quad (134)$$

$$\rightarrow -\frac{1}{2} \left\{ \boldsymbol{\Delta} \cdot \boldsymbol{\gamma} + m_c, m_c - \boldsymbol{\Delta}^{(2)} - \boldsymbol{\sigma} \cdot g\mathbf{F}/2 \right\} \quad (135)$$

using successive field transformations and obtain, in the last step, an operator that has only spatial derivatives.

The numerical results in this section suggest that these various strategies work about as well as expected, and that accurate simulations are possible with spatial lattice spacings between .3 and .4 fm. They also show that the meson dispersion relation (i.e., $c(\mathbf{p})$) at high and low momenta, the r -test and the ρ mass are all very sensitive to finite- a errors.

5 Heavy Quarks

As a final illustration of improved actions I briefly review techniques for simulating heavy quarks like the c and b quarks. Heavy quarks play a central role in the experimental study of weak interactions, and consequently it is important that we have reliable simulation techniques for their study. However heavy quark dynamics is not easily simulated using the quark actions of the previous section. Those actions only work well for quarks with energies and momenta small compared with the ultraviolet cutoff π/a . But heavy-quark hadrons have large rest energies (masses) and so necessitate small lattice spacings. Simulating an Υ , for example, using such techniques requires a lattice spacing of order $1/9.4 \text{ GeV} = .02 \text{ fm}$ or less—much too costly with today’s computers. Fortunately the heavy quarks are generally nonrelativistic in such mesons. Most of such a meson’s energy is due to the rest mass energy of its heavy-quark constituents, and rest mass energy plays little role in the dynamics of nonrelativistic particles. Consequently we can develop accurate simulation techniques that work well when the lattice spacing is chosen according to the size, rather than the mass, of the heavy-quark hadron: that is, for example, $a = .1 \text{ fm}$ rather than $.02 \text{ fm}$ for upsilons.¹³

Here I discuss only the NRQCD approach to heavy quark dynamics, where one takes maximum advantage of the fact that the heavy quarks are nonrelativistic [23]. I illustrate the technique by reviewing simulation results for the Υ and ψ families of mesons. These are attractive systems to study because so much is known already about them. The quark

¹³Actually since it is only the energy that is large, only the temporal lattice spacing need be small. Consequently the actions from the previous section can be used efficiently if one works with anisotropic lattices and small a_t ’s. Experiments using D234 actions are very encouraging [18]. Yet another approach to heavy-quark dynamics can be found in [22].

potential model, for example, provides an accurate phenomenological model of the internal structure of the mesons. Also there is much experimental data for these mesons. The low-lying states are largely insensitive to light-quark vacuum polarization — for example, the Υ , Υ' , $\chi_b \dots$ are all far below the threshold for decays into B mesons — and therefore can be accurately simulated with $n_f = 0$ light-quark flavors. Furthermore, these mesons are very small; for example, the Υ is about five times smaller than a light hadron. This makes them an excellent testing ground for our ideas concerning large lattice spacings.

Given that the heavy quarks are nonrelativistic, the most important momentum scales governing a heavy-quark meson's dynamics are smaller than the heavy quark's mass. We can take advantage of this fact by choosing an inverse lattice spacing of order the quark mass, thereby excluding relativistic states from the theory. Then it is efficient to analyze the heavy-quark dynamics using a nonrelativistic lagrangian (NRQCD). The lagrangian used to generate the results I show below was

$$\begin{aligned} \mathcal{L}_{\text{NRQCD}} &= \sum_x \left\{ \psi^\dagger(x+a_t\hat{t}) \left(1 - \frac{a_t H_0}{2n}\right)^n U_i^\dagger \left(1 - \frac{a_t H_0}{2n}\right)^n (1 - a_t \delta H) \psi(x) \right\} \\ &\quad - \sum_x \psi^\dagger(x) \psi(x), \end{aligned} \quad (136)$$

where $n = 2$, H_0 is the nonrelativistic kinetic-energy operator,

$$H_0 = -\frac{\Delta^{(2)}}{2M_0}, \quad (137)$$

M_0 is the bare heavy-quark mass, and δH is the leading relativistic and finite-lattice-spacing correction,

$$\begin{aligned} \delta H &= -\frac{(\Delta^{(2)})^2}{8M_0^3} \left(1 + \frac{a_t M_0}{2n}\right) + \frac{a_s^2 \Delta^{(4)}}{24M_0} \\ &\quad - \frac{g}{2M_0} \boldsymbol{\sigma} \cdot \mathbf{B} + \frac{ig}{8M_0^2} (\boldsymbol{\Delta} \cdot \mathbf{E} - \mathbf{E} \cdot \boldsymbol{\Delta}) \\ &\quad - \frac{g}{8M_0^2} \boldsymbol{\sigma} \cdot (\boldsymbol{\Delta} \times \mathbf{E} - \mathbf{E} \times \boldsymbol{\Delta}). \end{aligned} \quad (138)$$

Here \mathbf{E} and \mathbf{B} are the chromoelectric and chromomagnetic fields. As usual, the entire action is tadpole improved by dividing every link operator U_μ by u_0 . Potential models indicate that corrections beyond δH contribute only of order 5 MeV to Υ energies, and two or three times this for ψ 's.

The details of this lagrangian are unimportant to us here. What I want to focus on is the extent to which the improvement program outlined in earlier sections is effective for heavy-quark dynamics. The δH term consists of corrections just like the ones we have been analyzing for the other parts of QCD, the only difference here being that we are correcting both for finite- a and for the absence of relativity (ie, order v^2/c^2 errors). The coefficients of the correction terms were determined with tree-level perturbation theory and tadpole improvement, using precisely the techniques outlined in the earlier sections. The extent to which δH improves the simulation results is a measure of the efficacy of all the techniques discussed in these lectures.

Consider first a set of simulations of the Υ family that used a lattice spacing of about $1/12$ fm — roughly half the meson’s radius [24]. The spectrum is very well described by the simulations; results for the low-lying spectrum in different channels are shown in Figure 10. These compare well with experimental results (the horizontal lines), as they should since systematic errors are estimated to be less than 10–20 MeV. Two sets of Monte Carlo results are shown: one has no light-quark vacuum polarization, the other includes u and d quarks; as expected quark vacuum polarization has little effect on the spectrum. It is important to realize that these are calculations from first principles. The only inputs are the lagrangians describing gluon and quark dynamics, and the only parameters are the bare coupling constant and the bare quark mass. In particular, these results are not based on a phenomenological quark-potential model. These are among the most accurate lattice results to date.

The corrections in δH have only a small effect on the overall spectrum, but the spin structure is strongly affected. The lagrangian without δH is spin independent, and gives no spin splittings at all. Simulation results for the spin structure of the lowest lying P state are shown in Figure 11. Again these compare very well with the data, giving strong evidence that corrected lagrangians work. Systematic errors here are estimated to be of order 5 MeV. Note that the spin terms in δH all involve either chromoelectric or chromomagnetic field operators. These operators are built from products of four-link operators and so tadpole improvement increases their magnitude by almost a factor of two at the lattice spacing used here. Simulations without tadpole improvement give spin splittings that are much too small.

The correction terms also affect the extent to which the simulation reproduces continuum symmetries. For example, the low-momentum dispersion

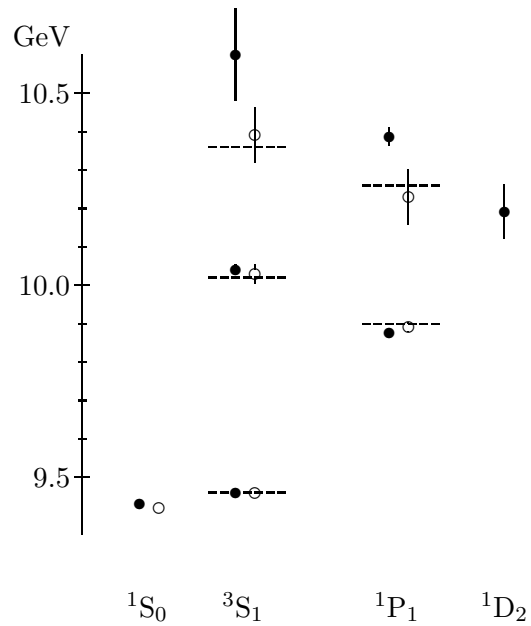


Figure 10: NRQCD simulation results for the spectrum of the $\Upsilon(^3S_1)$ and $h_b(^1P_1)$ and their radial excitations. Experimental values (dashed lines) are indicated for the S-states, and for the spin-average of the P-states. Simulation results are for $n_f=0$ (solid circles) and $n_f=2$ (open circles) light-quark flavors. The energy zero for the simulation results is adjusted to give the correct mass to the Υ .

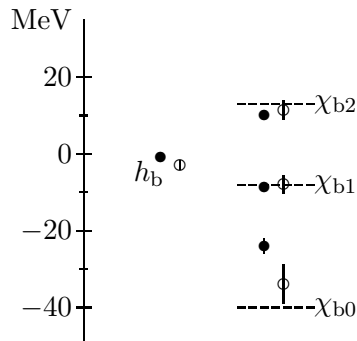


Figure 11: Simulation results for the spin structure of the lowest lying P-state in the Υ family. The dashed lines are the experimental values for the triplet states. Simulation results are for $n_f=0$ (solid circles) and $n_f=2$ (open circles) light-quark flavors.

relation of an upsilon in the simulation must have the form

$$E_\Upsilon(\mathbf{p}) = M_1 + \frac{\mathbf{p}^2}{2M_2} + \dots \quad (139)$$

In a relativistically invariant theory $M_1 = M_2$ is the upsilon mass. However in a purely nonrelativistic theory M_2 equals the sum of the quark masses, which differs from M_1 since M_1 also includes the quarks' binding energy. Only when relativistic corrections are added is M_2 shifted to include the binding energy. Simulations tuned to the correct mass $M_1 = 9.5(1)$ GeV give $M_2 = 8.2(1)$ GeV when δH is omitted. When δH is included, the simulations give $M_2 = 9.5(1)$ GeV, in excellent agreement with M_1 . All of the spin-independent pieces of δH contribute to the shift in M_2 ; once again we have striking evidence that corrected actions work.

This Υ simulation has only two parameters: the bare coupling constant and the bare quark mass. These were tuned until the simulation agreed with experimental data. From the bare parameters we can compute the renormalized coupling and mass. This simulation implies that the renormalized or “pole mass” of the b quark is [25]

$$M_b = 5.0(2) \text{ GeV}. \quad (140)$$

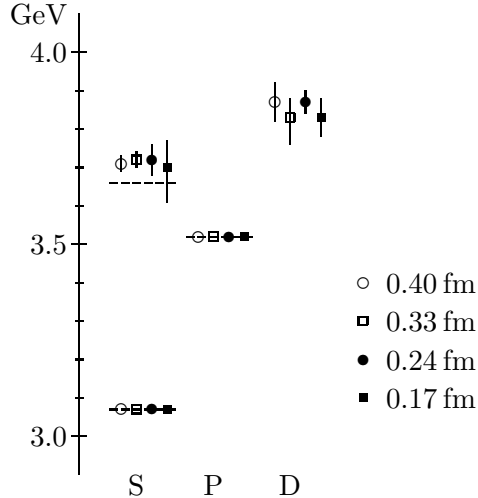


Figure 12: S, P and D states of charmonium computed on lattices with a range of lattice spacings. Improved quark and gluon actions were used in each case except $a = .17$ fm where only the quark action was improved.

The renormalized coupling that is obtained corresponds to [26]

$$\alpha_{\overline{\text{MS}}}^{(5)}(M_Z) = \begin{cases} .1175 (25) & \text{from } \chi_b - \Upsilon \text{ splitting} \\ .1180 (27) & \text{from } \Upsilon' - \Upsilon \text{ splitting} \end{cases} \quad (141)$$

depending upon which Υ splitting in the simulation is tuned to agree exactly with experiment. These values agree with results from high-energy phenomenology (but are more accurate). This last result is striking: it shows that the QCD of hadronic structure and the QCD of high-energy quark and gluon jets are really the same theory.

Another check on the corrected action is to show that results for physical quantities are independent of the lattice spacing. In Fig. 12 I show the low-lying spin-averaged spectrum of the ψ mesons computed using very coarse lattices, with a ranging from .17 fm to .40 fm [14]. The 1S and 1P masses are tuned; the 2S and 1D masses are predicted. The latter masses are independent of lattice spacing to within statistical errors of a few percent.

In Fig. 13 I show the 1S and 1P radial wavefunctions for charmonium, computed on lattices with two different lattice spacings using the (improved) NRQCD actions [14]. The most striking observation from these pictures is that the charge radius of the ψ is almost exactly equal to one lattice

spacing on the coarser lattice, and yet the results from the coarser lattice are essentially identical to those from the finer lattice. These data confirm that in general one needs only a few lattice points per direction within a hadron to obtain accurate results (few percent) from an a^2 -accurate action. Numerical experiments with the NRQCD action, where a^2 corrections are easily turned on and off, suggest that

$$r_{\text{hadron}} \approx a \Rightarrow \begin{cases} \mathcal{O}(a^2) \text{ corrections} \approx 15\text{--}20\% \\ \mathcal{O}(\alpha_s a^2, a^4) \approx 2\text{--}4\% \end{cases} \quad (142)$$

NRQCD simulations of heavy quarks were among the very first in which tadpole improvement played a crucial role. They remain among the best demonstrations of the technique.

Exercise: Verify that the continuum limit of the lattice NRQCD lagrangian (136) is a Schrödinger action with the standard relativistic corrections (chromomagnetic moment, Darwin term, spin-orbit coupling . . .).

6 Conclusions

Improved discretizations of QCD dynamics and large lattice spacings work. Tree-level (i.e., classical) improvement of the quark and gluon actions give results that are accurate to within a few to several percent for lattice spacings as large as .3–.4 fm, provided the all operators are tadpole-improved. Tree-level improvement is *not* surprisingly effective; it isn’t perfect. Rather, it works about as well as one would naively expect: there are certainly $\mathcal{O}(\alpha_s)$ corrections (and probably also nonperturbative corrections), and these will shift couplings by 10 or 20% and physical quantities by a few percent. That QCD simulations now conform to naive expectations and intuition is a major advance, perhaps *the* major advance. The current level of precision is more than sufficient to have a large impact on QCD phenomenology. And these techniques provide a firm foundation, a starting point, for future high-precision work that will rely upon some mixture of systematic perturbative calculations of the corrections, nonperturbative tuning, nontrivial transformations of the fields like those that lead to “perfect actions”, and perhaps analytic techniques like strong-coupling expansions.

The potential impact on QCD simulations of coarse lattices is enormous. This potential will be realized if lots of people become involved in the design, implementation and application this technology.

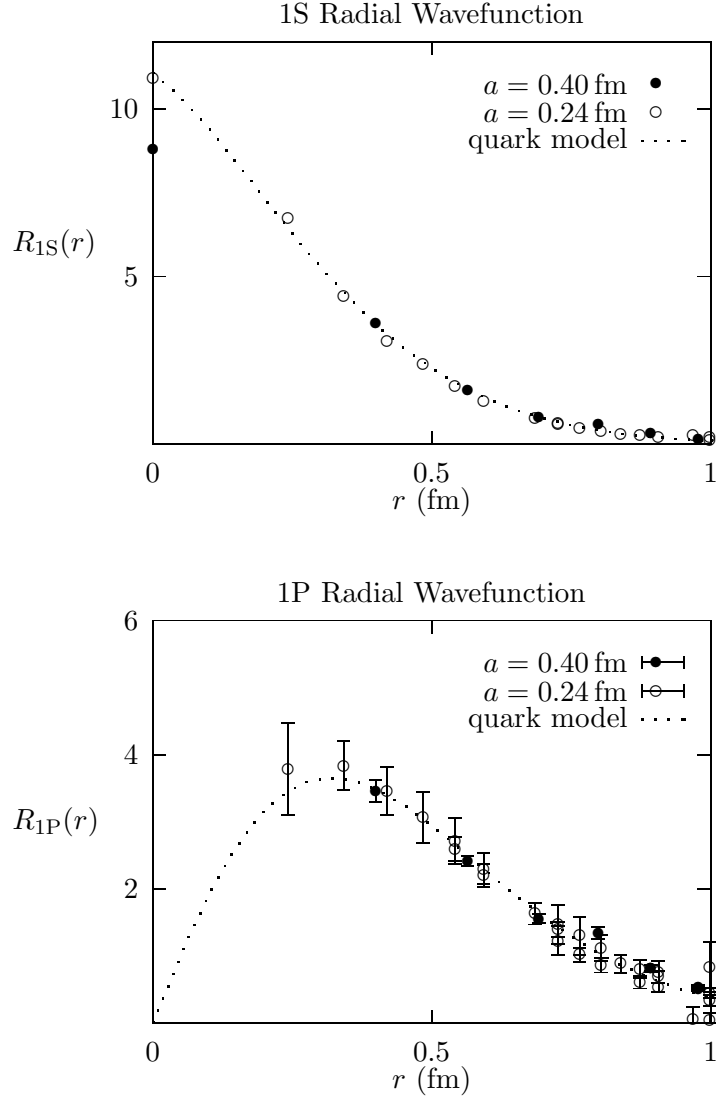


Figure 13: The radial wavefunctions for the 1S and 1P charmonium computed using improved actions and two different lattice spacings. Wavefunctions from a continuum quark model are also shown. Statistical errors are negligible for the 1S wavefunction.

References

- [1] M. Creutz, *Quarks, gluons and lattices* (Cambridge University Press, Cambridge, 1985).
- [2] I. Montvay and G. Münster, *Quantum Fields on a Lattice* (Cambridge University Press, Cambridge, 1994).
- [3] G.P. Lepage, "The Analysis of Algorithms for Lattice Field Theory" in *From Actions to Answers*, edited by T. DeGrand and D. Toussaint (World Scientific, Singapore, 1989).
- [4] K. Symanzik, *Nucl. Phys.* **B226** (1983) 187.
- [5] G.P. Lepage and P.B. Mackenzie, *Phys. Rev.* **D48** (1993) 2250.
- [6] For an overview see K.G. Wilson, *Rev. Mod. Phys.* **55** (1983) 583.
- [7] G.P. Lepage, *Lattice QCD for Small Computers* in *The Building Blocks of Creation*, edited by S. Raby and T. Walker (World Scientific Press, Singapore, 1994).
- [8] See, for example, H. Kawai, R. Nakayama and K. Seo, *Nucl. Phys.* **B189** (1981) 40.
- [9] P. Hasenfratz and F. Niedermayer, *Nucl. Phys.* **B414** (1994) 785.
- [10] T. DeGrand, A. Hasenfratz, P. Hasenfratz and F. Niedermayer, *Phys.Lett.* **B365** (1996) 233; *Nucl.Phys.* **B454** (1995) 587; *Nucl.Phys.* **B454** (1995) 615.
- [11] W. Bietenholz and U.J. Wiese, *Nucl.Phys.* **B464** (1996) 319.
- [12] G. Curci, P. Menotti, and G. Paffuti, *Phys. Lett.* **130B** (1983) 205; Erratum: *ibid.* **135B** (1984) 516.
- [13] M. Lüscher and P. Weisz, *Comm. Math. Phys.* **97** (1985) 59.
- [14] M. Alford, W. Dimm, G.P. Lepage, G. Hockney and P. Mackenzie, *Phys. Lett.* **B361** (1995) 87.
- [15] M. Lüscher and P. Weisz, *Phys. Lett.* **158B**, (1985) 250, and references therein.

- [16] D.W.Bliss, K.Hornbostel and G.P.Lepage, hep-lat-9605041 preprint (1996).
- [17] B.Sheikholeslami and R.Wohlert, *Nucl.Phys.* **B259** (1985) 572.
- [18] M.Alford, T.Klassen and G.P.Lepage, *Nucl. Phys.* **B47** (Proc. Suppl.) (1996) 370; and talks by M.Alford and T.Klassen at *Lattice '96* (June 1996, St. Louis).
- [19] K.Jansen, C.Liu, M.Lüscher, H.Simma, S.Sint, R.Sommer, P.Weisz and U.Wolff, *Nucl.Phys.* **B372** (1996) 275; and R.Sommer's talk at *Lattice '96* (June 1996, St. Louis).
- [20] S.Collins, R.G.Edwards, U.M.Heller and J.Sloan *Nucl. Phys.* **B47** (Proc. Suppl.) (1996) 366; and R.G.Edward's talk at *Lattice '96* (June 1996, St. Louis).
- [21] F.Butler, H.Chen, J.Sexton, A.Vaccarino and D.Weingarten, *Nucl.Phys.* **B430** (1994) 179.
- [22] A.X.El-Khadra, A.S.Kronfeld and P.B.Mackenzie, Fermilab preprint hep-lat/9604004 (April, 1996).
- [23] G.P.Lepage and B.Thacker, *Nucl. Phys.* **B**(Proc. Suppl.)**4** (1988) 199; G.P.Lepage, K.Hornbostel, L.Magnea, U.Magnea and C.Nakhleh, *Phys. Rev.* **D46** (1992) 4052.
- [24] C.Davies et al., *Phys. Rev.* **D50** (1994) 6963; P.McCallum and J.Shigemitsu, *Nucl. Phys.* **B47** (Proc. Suppl.) (1996) 409.
- [25] C.Davies et al., *Phys. Rev. Lett.* **73** (1994) 2654.
- [26] C.Davies et al., *Phys. Lett.* **B345** (1995) 42; J.Shigemitsu's talk at *Lattice '96* (June 1996, St. Louis).